Longitudinal map of transcriptome changes in the Lyme pathogen *Borrelia burgdorferi* during tick-borne transmission

Anne L. Sapiro[1*], Beth M. Hayes[1], Regan F. Volk[2], Jenny Y. Zhang[1], Diane M. Brooks[3], Calla Martyn[1], Atanas Radkov[1], Ziyi Zhao[1], Margie Kinnersley[3], Patrick R. Secor[3], Balyn W. Zaro[2], Seemay Chou[1*]

1 Department of Biochemistry & Biophysics, University of California, San Francisco, California, USA
2 Department of Pharmaceutical Chemistry and Cardiovascular Research Institute, University of California, San Francisco, California, USA
3 Division of Biological Sciences, University of Montana, Missoula, Montana, USA

*Corresponding authors:
Anne L. Sapiro: annesapiro@gmail.com & Seemay Chou: seemaychou@gmail.com

ABSTRACT

Borrelia burgdorferi (*Bb*), the causative agent of Lyme disease, adapts to vastly different environments as it cycles between tick vector and vertebrate host. During a tick bloodmeal, *Bb* alters its gene expression to prepare for vertebrate infection; however, the full range of transcriptional changes that occur over several days inside of the tick are technically challenging to capture. We developed an experimental approach to enrich *Bb* cells to longitudinally define their global transcriptomic landscape inside nymphal *Ixodes scapularis* ticks during a transmitting bloodmeal. We identified 192 *Bb* genes that substantially change expression over the course of the bloodmeal from one to four days after host attachment. The majority of upregulated genes encode proteins found at the cell envelope or proteins of unknown function, including 45 outer surface lipoproteins embedded in the unusual protein-rich coat of *Bb*. As these proteins may facilitate *Bb* interactions with the host, we utilized mass spectrometry to identify candidate tick proteins that physically associate with *Bb*. The *Bb* enrichment methodology along with the *ex vivo* *Bb* transcriptomes and candidate tick interacting proteins presented here provide a resource to facilitate investigations into key determinants of *Bb* priming and transmission during the tick stage of its unique transmission cycle.

INTRODUCTION

Vector-borne microbial pathogens are transmitted by the bite of arthropods and have evolved sophisticated ways to adapt to vastly different environments as they move between vector and host. Uncovering their adaptive mechanisms can not only open avenues for disrupting pathogen transmission but also provide fundamental insights into vector physiology and microbial symbioses (Shaw and Catteruccia, 2018). Lyme disease, the most reported vector-borne disease in North America, is caused by the bacterial pathogen *Borrelia burgdorferi* (*Bb*) (Rosenberg et al., 2018; Steere et al., 2016). Its primary vector, the blacklegged tick *Ixodes scapularis,* acquires and transmits *Bb* through two separate multi-day bloodmeals, one in which *Bb* is acquired from an infected vertebrate host and a second, during the subsequent life stage, in which *Bb* is transmitted to a new host (Tilly et al., 2008). During the transmission bloodmeal, *Bb* proliferate in the tick midgut before a subset of these cells disseminate to the salivary glands (Dunham-Ems et al., 2009). *Bb* is deposited into the new host via the tick saliva extruded into the bite site (Spielman et al., 1987). Given the prolonged nature of *I. scapularis* feeding, the high specificity of vector-pathogen relationships, and the complicated array of events needed for successful *Bb* transmission, the tick bloodmeal provides an opportune intervention point for preventing pathogen spread. However, we do not currently have a clear understanding of the molecular mechanisms involved in this process.

Bb must adapt to dramatically different environments as it cycles from tick to vertebrate host, and understanding the genes involved in this process will enable the identification of key interactions to target to prevent transmission. When an infected tick feeds, *Bb* responds to bloodmeal-induced environmental changes and undergoes cellular modifications driven by key transcriptional circuits, including the RpoN-RpoS sigma factor cascade and the Hk1/Rrp1 two-component system (Radolf et al., 2012). *In vitro* analyses of *Bb* cells cultured in tick- or mammal-like growth conditions have pointed to additional genetic determinants of tick-borne transmission by revealing widespread transcriptome remodeling during host switching (reviewed in Samuels et al., 2021). However, it is not fully clear how these *in vitro* expression changes correspond to complex *in vivo* changes over the course of a transmission bloodmeal. Capturing comprehensive, longitudinal data on *Bb* gene expression from inside its vector has been hampered by technical challenges due to the dynamic nature of the bloodmeal and the general low abundance of bacterial cells relative to the tick (Samuels et al., 2021). Some progress has been made in making transcriptome-wide measurements from the tick. *Bb* sequence enrichment coupled with microarrays identified large scale changes in *Bb* gene expression between the first and second tick bloodmeals (Iyer et al.,

2015). More recently, enriching *Bb* sequences from infected tick RNA-seq libraries through TDBCapSeq has provided clearer resolution into differences in *Bb* gene expression as it cycles between the fed tick and mammalian host (Grassmann et al., 2023). Still, we have limited temporal resolution into the molecular transitions that happen across key steps of tick feeding. This problem necessitates novel approaches to capture the transcriptomic changes of *Bb* within the natural tick environment.

While the full landscape of *Bb* transmission determinants is not yet known, we do have a growing knowledge of functional processes that are critical during the tick stage, such as motility, metabolism, and immune evasion (Kurokawa et al., 2020; Phelan et al., 2019). These functions often rely on the unique protein-rich *Bb* outer surface. Notably, several specific tick–*Bb* protein–protein interactions are important for *Bb* survival, migration, or transmission to the next host. *Bb* encodes an extensive outer surface protein (Osp) family with members that are differentially expressed during host switching. One of these proteins, OspA, binds a tick cell surface protein, tick receptor for OspA (TROSPA), which is required for successful *Bb* colonization of the tick midgut during the first acquisition bloodmeal (Pal et al., 2004). Several other proteins have also been linked to *Bb* migration within the tick (Pal et al., 2021). For example, BBE31 binds a tick protein TRE31, and disruption of this interaction decreases the number of *Bb* cells that successfully migrate from the tick gut to salivary glands (Zhang et al., 2011). However, these interactions alone are not sufficient to block *Bb* growth or migration in ticks, suggesting there are likely additional molecular factors from *Bb* and ticks at play during tick-borne transmission.

To provide a more comprehensive set of *Bb* determinants driving tick-borne transmission of this important human pathogen, we developed a novel sequencing-based strategy for *ex vivo* transcriptomic profiling of *Bb* populations within infected nymphal *I. scapularis* ticks as they transmit *Bb* to a mouse host. We used this method to longitudinally map genome-wide *Bb* expression changes for bacterial cells isolated from inside ticks during the transmission bloodmeal from one to four days after attachment. We identified 192 highly differentially expressed genes, including genes previously implicated in *Bb* transmission as well as many others. Genes upregulated during tick transmission were enriched for outer surface lipoproteins, suggesting *Bb* dramatically remodels its cell envelope as it migrates through the tick. Mass spectrometry analyses revealed dramatic changes in the tick environment over feeding, identifying new potential determinants of a more extensive and diverse set of tick–microbe molecular interactions than previously appreciated. The *Bb* enrichment method and resulting datasets provide an

important community resource to facilitate further investigations into the key determinants of *Bb* transmission.

RESULTS

A two-step enrichment process facilitates robust transcriptional profiling of *Bb* during the tick bloodmeal

To gain a more comprehensive understanding of *Bb* gene expression throughout the tick phase of the transmission cycle, we developed an experimental approach to characterize the *Bb* transcriptome of spirochetes isolated from nymphal *I. scapularis* ticks during a days-long bloodmeal in which *Bb* is transmitted to a vertebrate host. We aimed to establish a longitudinal transcriptional profile encompassing key pathogen transmission events each day of feeding after ticks attached to their mouse bloodmeal hosts (**Figure 1A**). We fed *Bb*-infected nymphal ticks on naïve mice and collected the feeding ticks at daily intervals after the start of feeding until four days after attachment, at which time the ticks had fully engorged and detached from the mice. The major bottleneck for such an RNA sequencing (RNA-seq) approach is capturing sufficient quantities of *Bb* transcripts from complex multi-organism samples in which pathogen transcripts represent a very small minority. Our initial attempts to uncover *Bb* mRNA by simply removing tick mRNA with polyA-depletion and removing tick rRNA sequences using Depletion of Abundant Sequences by Hybridization (DASH) (Dynerman et al., 2020; Gu et al., 2016) were unsuccessful. This approach resulted in an average of only 0.09% of RNA-seq reads mapping to *Bb* mRNA – approximately 10-fold less than we estimated would be needed to feasibly obtain robust transcriptome-wide differential gene expression analysis (Haas et al., 2012).

To dramatically increase *Bb* transcript representation in our libraries, we physically enriched *Bb* cells in tick lysates prior to library preparation by adding an initial step of immunomagnetic separation (**Figure 1B**). We took advantage of a commercial antibody previously generated

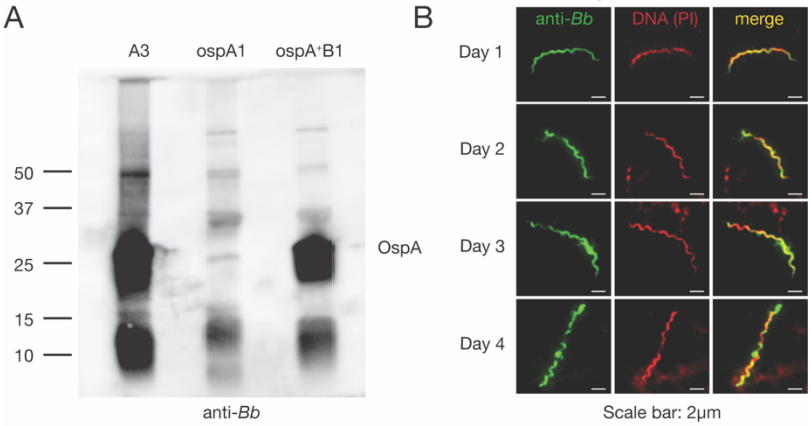

Figure S1. α*Bb* antibody recognizes OspA and binds *Bb* in the tick throughout the bloodmeal. (**A**) Western blot with α*Bb* on lysate from cultured *Bb*: wildtype (A3, left), a mutant lacking *ospA* (ospA1), and the mutant with *ospA* restored (ospA+B1)(Battisti et al., 2008). α*Bb* recognizes OspA among other proteins. (**B**) Immunofluorescence microscopy with α*Bb* (green, left) and propidium iodide (PI) (DNA, red, center) on each day of feeding (merge is yellow, right). α*Bb* antibody recognizes *Bb* in the tick across the bloodmeal.

136 against whole *Bb* cells (α*Bb*, RRID: AB_1016668). By western blot analysis, we confirmed that
137 α*Bb* specifically recognized several *Bb* proteins, including surface protein OspA (**Figure S1A**),

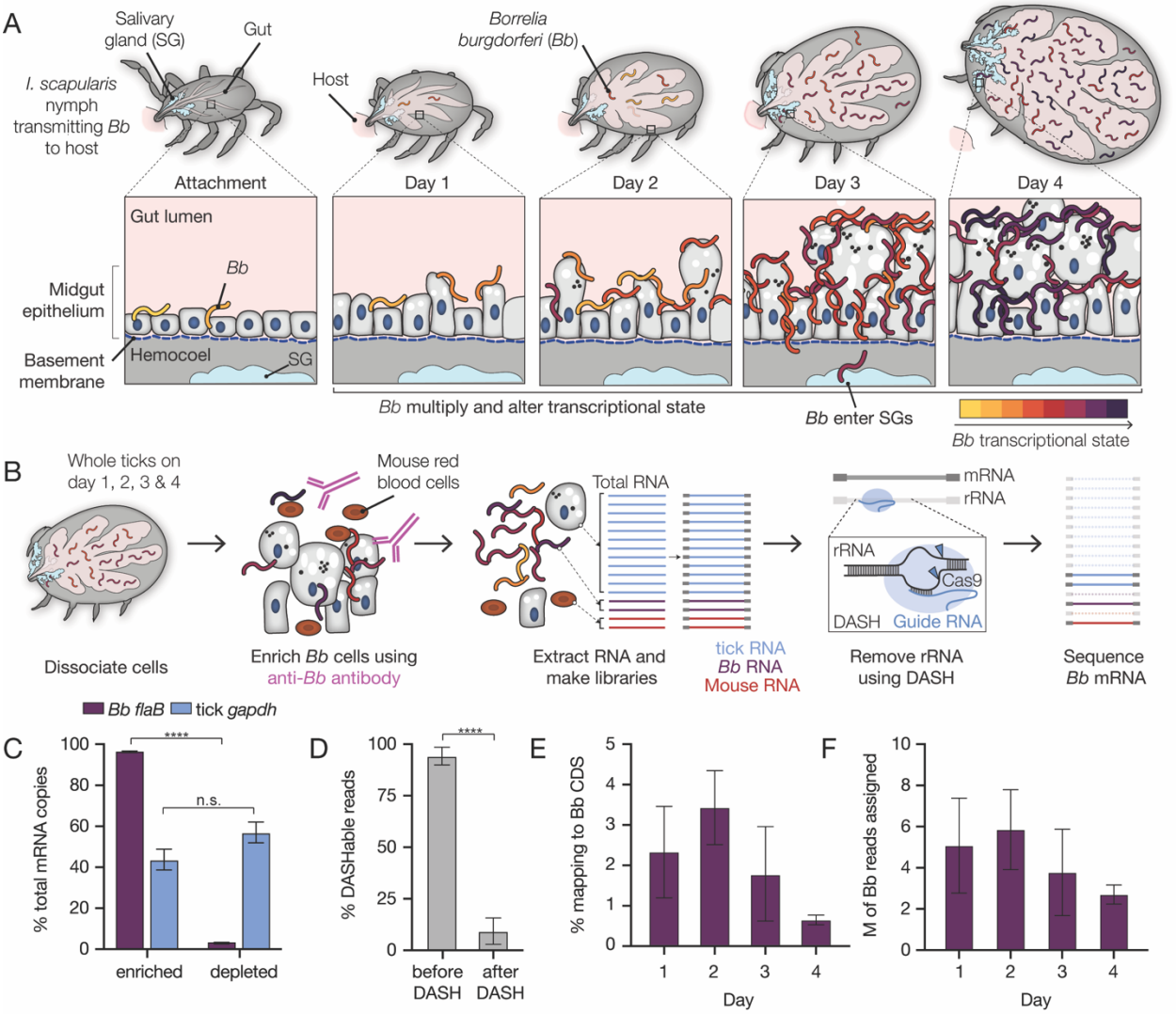

Figure 1. A two-step enrichment process facilitates robust transcriptional profiling of *Bb* during the tick bloodmeal. (**A**) Schematic of *Bb* during nymphal *I. scapularis* feeding. *Bb* in the nymphal tick midgut respond to the nutrient-rich bloodmeal by multiplying and changing their transcriptional state (Ouyang et al., 2012; de Silva and Fikrig, 1995). At the same time, the tick gut undergoes numerous changes to digest the bloodmeal (Caimano et al., 2015; Sonenshine and Anderson, 2014). After two to three days of feeding, a small number of *Bb* leave the midgut and enter the salivary glands (blue), while the majority are left behind in the gut after engorgement (Dunham-Ems et al., 2009). (**B**) Schematic of *Bb* enrichment process from feeding ticks. Whole ticks are dissociated, α*Bb* antibodies are added to lysates, and antibodies and *Bb* are captured magnetically. RNA is extracted and RNA-seq libraries are prepared. DASH is then used to remove rRNA before sequencing. This process increases *Bb* reads in the resulting sequencing data. (**C**) RT-qPCR results showing the percentage of *Bb flaB* and *I. scapularis gapdh* RNA in the enriched versus depleted fractions after the enrichment process. Data come from 4 replicates each from day 2, day 3, and day 4, mean +/- SE. ****p-value<0.0001, paired t test. Nearly all *Bb flaB* RNA was found in the enriched fraction. (**D**) The percentage of reads mapping to rRNA before and after DASH. n=4. Data are shown as mean +/- SD. ****p-value<0.0001, paired t test. rRNA reads are drastically reduced after DASH. (**E**) The percentage of reads in RNA-seq libraries mapping to *Bb*. *Bb* mRNA reads make up a larger proportion of libraries than without enrichment. Data are shown as mean +/- SD. (**F**) The number of reads in millions (M) mapped to *Bb* for each day. n=4. Data are shown as mean +/- SD. An average of 4.3 million reads per sample mapped to *Bb* genes, covering 92% of genes with at least 10 reads.

138 which is highly prevalent on the *Bb* surface in the tick (Radolf et al., 2012). In addition,
139 immunofluorescence microscopy with α*Bb* showed clear recognition of *Bb* cells from within the
140 tick at each day of feeding (**Figure S1B**). After collecting infected nymphal ticks from mice one,
141 two, three, and four days post-attachment, we used α*Bb* and magnetic beads to enrich *Bb* cells
142 from the tick material in the lysates. We tracked relative *Bb* enrichment through RT-qPCR of *Bb*
143 *flaB* RNA and tick *gapdh* RNA in the separated samples. Measuring *Bb flaB* RNA from both *Bb*-
144 enriched samples and their matched *Bb*-depleted fractions, we found over 95% of total *Bb flaB*
145 RNA was present in enriched fractions (**Figure 1C**), suggesting our approach captured the vast
146 majority of *Bb* transcripts from the tick.
147
148 Total RNA recovered from the enrichment process was used to create RNA-seq libraries that
149 subsequently underwent depletion of rRNA sequences from the tick, mouse, and *Bb* using DASH,
150 which targets unwanted sequences for degradation by Cas9 (Gu et al., 2016; Ring et al., 2022).
151 DASH reduced unwanted sequences from 94% to 9% of our total libraries, greatly increasing the
152 relative abundance of *Bb* transcripts (**Figure 1D**). For resulting libraries generated across feeding,
153 between 0.6% and 3.4% of reads mapped to *Bb* coding regions (**Figure 1E**), which translated to
154 an average of 4.3 million *Bb* genic reads per sample (**Figure 1F** and **Table S1**).
155
156 As expected, for samples pulled from the mice one, two, and three days after attachment, the
157 majority of the remaining sequencing reads mapped to the *I. scapularis* genome (72-83%) (**Table**
158 **S1**). On day four, when ticks were fully engorged and were recovered from mouse cages rather
159 than pulled from the mice, we found that fewer reads mapped to the *I. scapularis* genome (24-
160 44%). Only a small percentage of reads from all samples mapped to the host *Mus musculus*
161 genome (1-3%). To identify the source of the remaining reads in the day 4 samples, we ran the
162 data through a publicly available computational pipeline that identifies microbes in sequencing
163 datasets, CZ ID (Kalantar et al., 2020). This analysis led us to discover that a large percentage of
164 day 4 reads mapped to bacterial species *Pseudomonas fulva* (41-64%) (**Table S1**), which may
165 have been present in our mouse cages. While these samples had a lower percentage of reads
166 that mapped to *Bb*, broad transcriptome coverage was still obtained by increasing total
167 sequencing depth. Across all samples, at least 10 reads mapped to 92% of *Bb* genes. The median
168 number of reads per gene in each sample varied from 338 to 1167 reads (**Table S1**). This
169 coverage was sufficient for statistically significant downstream differential expression analyses
170 for the vast majority of *Bb* genes.
171

172 To evaluate whether our approach introduced any major
173 artifacts in *Bb* expression, we sequenced and compared
174 RNA-seq libraries from *in vitro* cultured *Bb* cells before and
175 after immunomagnetic enrichment. We found minimal
176 expression differences (29 genes with p<0.05, fold changes
177 between 0.83-1.12) (**Figure S2** and **Table S2**), suggesting
178 experimental enrichment did not significantly alter global
179 transcriptome profiles for *Bb*. Thus, our enrichment
180 approach enabled genome-wide analysis of *Bb* population-
181 level expression changes that occur within the feeding
182 nymph as *Bb* is transmitted to the host.

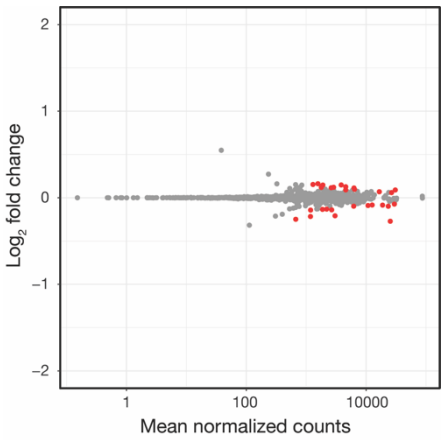

Figure S2. Enrichment process does not induce large scale gene expression changes in *in vitro* cultured *Bb*. Log_2 fold changes vs. mean normalized number of counts comparing cultured *Bb* input and samples after enrichment with α*Bb*. n=3. Red dots, p-value < 0.05, Wald tests. The gene expression changes induced during processing are much smaller than those observed between days of feeding.

183

184 **Global *ex vivo* profiling of *Bb* reveals extent and**
185 **kinetics of transcriptional changes**

186 To provide a broad overview of *Bb* expression changes in
187 the tick during the nymphal *I. scapularis* transmission
188 bloodmeal, we performed principal component analysis (PCA) on the *Bb* transcriptome data from
189 one, two, three, and four days after attachment (n=4). We reasoned that if many longitudinal
190 expression changes were occurring across *Bb* populations, we would observe greater data
191 variability between time points than between biological replicates. Indeed, we found replicates
192 from each day grouped together, whereas distinct time points were largely non-overlapping. The
193 first principal component, which explained 64% of the variance in our data, correlated well with
194 day of feeding (**Figure 2A**). The global pattern suggested that *Bb* gene expression changes
195 generally trended in the same direction over the course of feeding with the most dramatic
196 differences between flanking timepoints on day 1 and day 4.

197

198 Using day 1 (early attachment) as a baseline, we performed differential expression analysis for
199 all *Bb* genes at subsequent time points (day 2, day 3, day 4) (**Figure 2B** and **Table S3**). We
200 examined changes with p-values < 0.05 when adjusted for multiple hypothesis testing and fold
201 changes above a two-fold threshold (listed in **Table S4**). These analyses mirrored the global
202 longitudinal expression pattern predicted by the PCA. The total number of differentially expressed
203 (DE) genes when compared to day 1 increased with each subsequent timepoint to day 4. By day
204 4 there were 186 DE genes, including 153 upregulated and 33 downregulated (**Figure 2C-E**).
205 Across all later time point comparisons to day 1, DE genes were highly overlapping and largely

206 changed in the same directions. For example, of the DE genes that increased on day 2, 29 of 30
207 were still increased on day 3, and 29 of 30 were still increased on day 4. In the day 2, day 3, and
208 day 4 comparisons to the day 1 baseline, we found 192 DE genes in total (**Table S4**). There were
209 some notable differences between genes, such as the overall timing and kinetics of expression
210 changes. Transcript levels for some DE genes changed suddenly over the course of feeding,
211 while others were more gradual. To our knowledge, this is the first comprehensive report of global
212 *Bb* expression changes over multiple stages of a tick feeding.

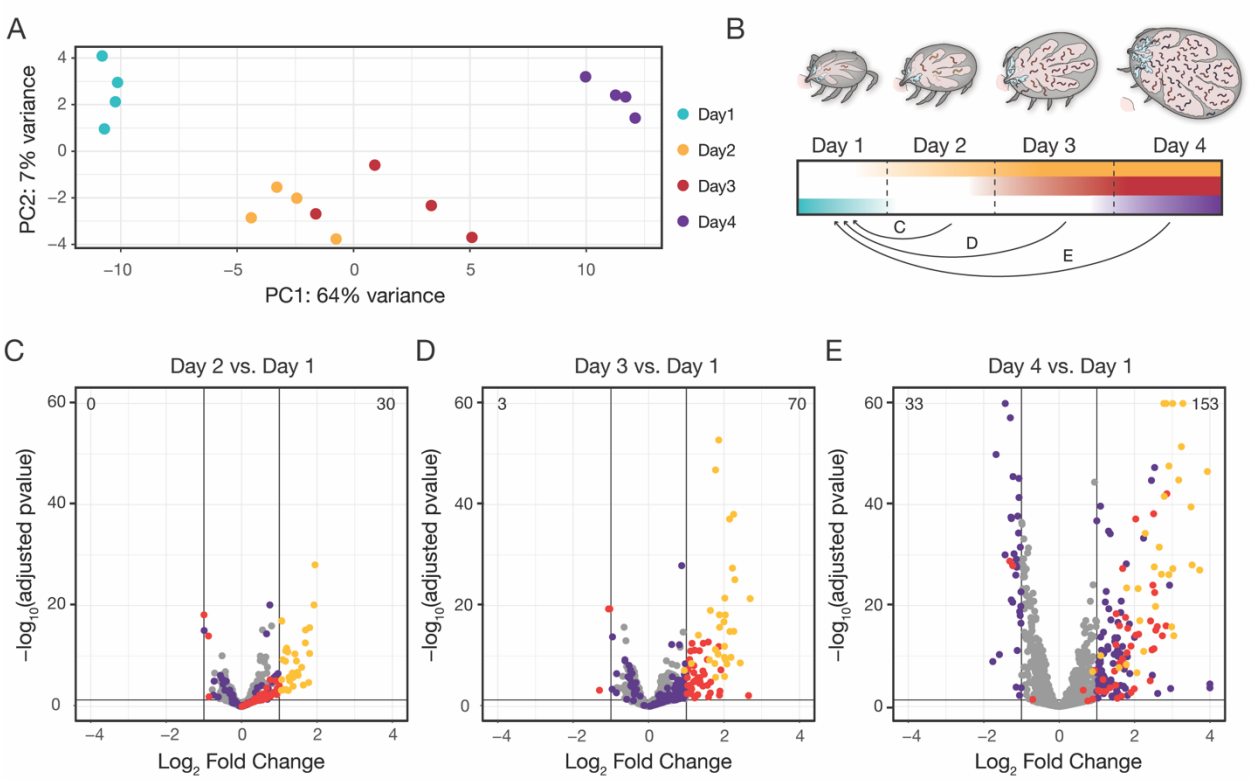

Figure 2. Global *ex vivo* profiling of *Bb* reveals extent and kinetics of transcriptional changes. (**A**) Principal component analysis of samples from across feeding. PC1 correlates strongly with day of feeding. (**B**) Schematic depicting how data was analyzed, as pairwise comparisons between the first day after attachment and all other days. (**C-E**) Volcano plots of differentially expressed genes comparing day 2 versus day 1(**C**), day 3 versus day 1 (**D**), and day 4 versus day 1 (**E**). The total number of upregulated genes is shown in the top right and the number of downregulated genes is shown in the top left. Yellow dots are genes that first change expression between day 1 and day 2, red dots are genes that first change expression between day 1 and day 3, and purple dots are genes that first change expression between day 1 and day 4. Two genes with $\log_2$ fold changes >4 are shown at x=4, and five genes with $-\log_{10}$(padj) >60 are shown at y=60. Only genes with p-value < 0.05 from Wald tests and at least a two-fold change are highlighted. n=4. By day 4 of feeding, 153 genes are upregulated and 33 genes are downregulated from day 1 baseline levels.

213

214 To assess the integrity of our dataset, we first examined expression profiles of previously
215 characterized targets of major transcriptional programs activated at the onset of the bloodmeal:
216 the RpoN/RpoS sigma factor cascade and the Hk1/Rrp1 two-component system (Caimano et al.,

2015; Grassmann et al., 2023). Between day 1 and day 4, the expression of *rpoS* increased (**Figure S3A**), as expected (Hübner et al., 2001), and the majority of genes activated by RpoS in the feeding tick (Grassmann et al., 2023), including canonical targets *ospC* and *dbpA*, were also significantly upregulated (79/89, p<0.05, Wald tests) (**Figure S3B**). The majority of genes activated or repressed by Rrp1 *in vitro* (Caimano et al., 2015) also trended significantly in the expected direction *ex vivo* between day 1 and day 4 (111/148 upregulated, 37/57 downregulated, p<0.05, Wald tests, **Figure S3C**). We also examined the expression trends of genes regulated by Rel_{Bbu} as part of the stringent response, another major transcriptional program active in *Bb* in the tick during nutrient starvation (Drecktrah et al., 2015). About half of Rel_{Bbu}-regulated genes changed in the direction expected if the stringent response was active during this time (129/251 upregulated, 111/226 downregulated, p<0.05, Wald tests) (**Figure S3D**); however, more of the genes that were two-fold downregulated over feeding are regulated by Rel_{Bbu} than either RpoS or Rrp1, suggesting it may play a role during this time frame.

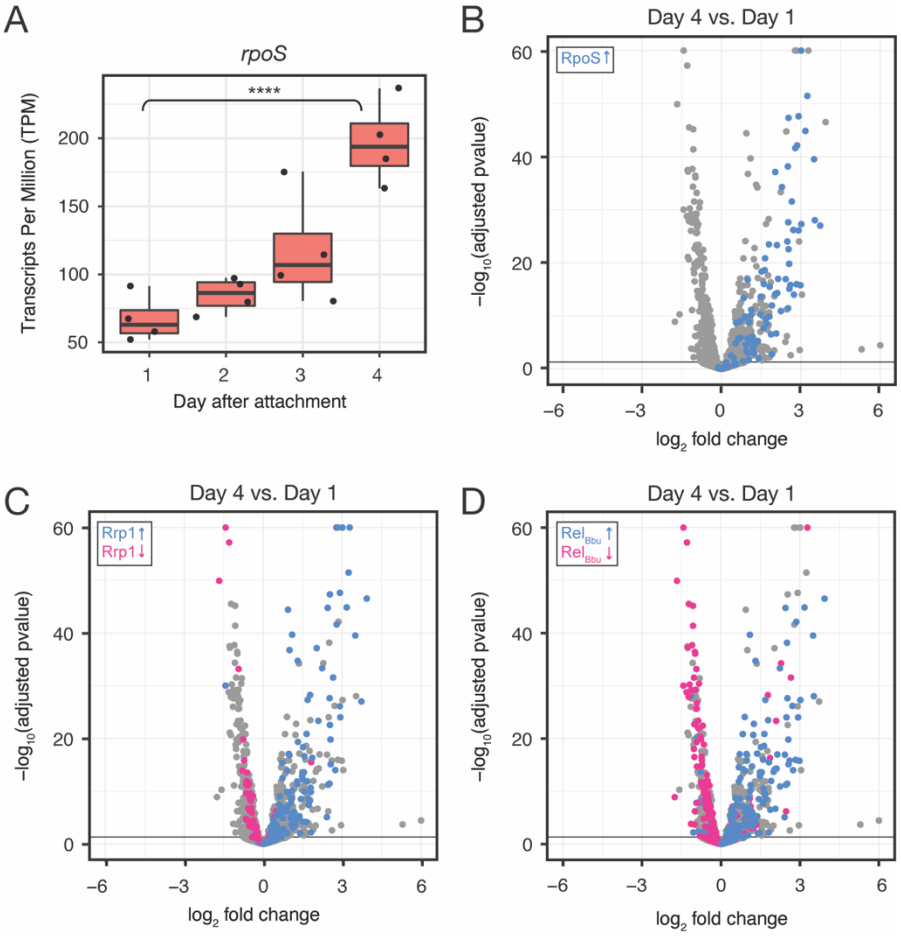

Figure S3. *Ex vivo* RNA-seq corroborates transcriptional programs in the tick. (A) Tukey style boxplot of Transcripts Per Million (TPM) on each day for *rpo*S. Black dots represent replicates. ****p-value < 0.00001, Wald test. *rpoS* expression increases over the course of feeding. (**B**) Volcano plot of DE genes comparing day 4 to day 1, with RpoS-upregulated genes (blue). Genes upregulated by RpoS in ticks increase during feeding. (**C**) Volcano plot of DE genes comparing day 4 to day 1, with Rrp1-upregulated (blue) and downregulated (pink) genes. Rrp1-regulated genes correlate well with genes up and downregulated during feeding. (**D**) Volcano plot of DE genes comparing day 4 to day 1, with Rel_{Bbu}-upregulated (blue) and downregulated (pink) genes. About half of Rel_{Bbu} genes change in the expected direction over feeding.

231 We then compared the 192 two-fold DE genes in our longitudinal time course to those identified
232 in two previous studies that measured *Bb* gene expression changes from culture conditions
233 approximating the unfed tick and fed tick through modulation of temperature and/or pH (Ojaimi et
234 al., 2003; Revel et al., 2002). 31% of the DE genes upregulated from day 1 (49/158) were more
235 highly expressed in "fed tick" conditions compared to "unfed tick" conditions in one or both studies,
236 while 24% of the DE genes downregulated from day 1 (8/24) were more highly expressed in
237 "unfed tick" conditions in one or both studies (**Figure S4A** and **Table S4**). The studies become
238 more concordant when focusing on the DE genes that were upregulated on day 2, which were
239 generally the genes that changed the most dramatically in the time course. 70% of DE genes
240 upregulated on day 2 (21/30) were more highly expressed in "fed tick" conditions in these previous
241 studies, suggesting that the majority of the most dramatic gene expression changes we saw
242 across feeding agree with what was observed in these previous studies.

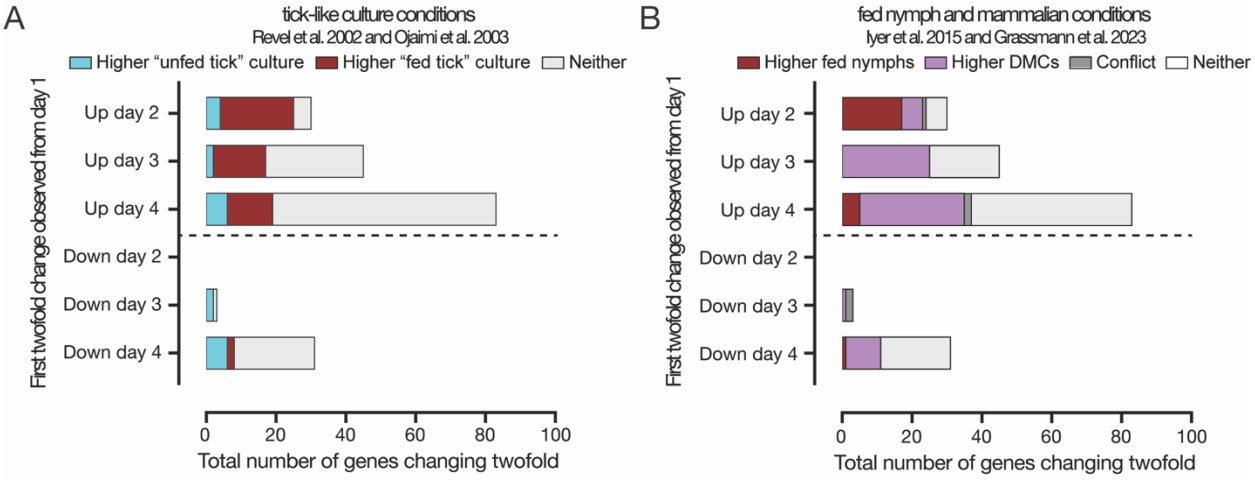

Figure S4. Genes changing over tick feeding overlap with genes that change expression in previously probed tick feeding contexts. (**A**) The overlap of two-fold changed genes with genes that changed expression in *Bb* cultures grown in conditions mimicking feeding ticks. Genes are grouped based on the first day that they changed two-fold from day 1. "Fed tick" culture conditions were 37ºC, pH 6.8 in Revel et al. 2002 and 35ºC, pH 7.4 in Ojaimi et al. 2003, and genes elevated in these conditions in one or both studies are highlighted in red. "Unfed tick" culture conditions were 23ºC, pH 7.5 in Revel et al. 2002 and 23ºC, pH 7.4 in Ojaimi et al. 2003, and genes elevated in these conditions in one or both studies are highlighted in teal. Genes that were not elevated in either condition in those studies are in gray. Particularly for genes that increase on day 2, there is a large overlap with genes elevated in "fed tick" culture conditions in previous studies. (**B**) The overlap of two-fold changed genes with genes that changed expression between fed nymphs and dialysis membrane chambers (DMCs) mimicking mammalian conditions. Genes are grouped based on the first day that they changed two-fold from day 1. *Bb* expression in fed nymphs versus in DMCs was compared by Iyer et al. 2015 using bacterial RNA amplification and microarray, while Grassmann et al. 2023 used TBDCapSeq. Genes elevated in fed nymphs in one or both studies are highlighted in red, while genes elevated in DMCs in one or both studies are highlighted in purple. Genes that were elevated in conflicting conditions between the two studies are in dark gray, while genes not elevated in either condition are in light gray. For genes that increase on day 2, there is a large overlap with genes elevated in fed nymphs, while genes that increase first on days 3 and 4 have a larger overlap with genes elevated in DMCs.

243

244 We also compared the DE genes to two studies that assessed *Bb* gene expression differences in
245 fed nymphs versus dialysis membrane chambers (DMCs), which mimic *Bb* conditions in the

246 mammal (Grassmann et al., 2023; Iyer et al., 2015). 63% of all upregulated DE genes (100/158)
247 were differentially expressed between fed nymphs and DMCs in one or both studies (**Figure S4B**
248 and **Table S4**). The genes that were more highly expressed in nymphs were most concentrated
249 amongst the day 2 DE genes (17/30, 57%), while the genes more highly expressed in DMCs were
250 concentrated amongst the day 3 and day 4 DE genes (55/128, 43%). These comparisons
251 suggested that the timing and magnitude of gene expression changes during feeding may indicate
252 whether gene expression will peak in the tick or continue rising once *Bb* is transmitted to the host.
253
254 Through comparisons to these previous studies, we were able to verify that our data captured
255 many expected transcriptional trends occurring during tick feeding. Nevertheless, 14% of the two-
256 fold DE genes were not previously found to change expression in these different tick-feeding
257 contexts (Grassmann et al., 2023; Iyer et al., 2015; Ojaimi et al., 2003; Revel et al., 2002) or
258 identified in these RNA-seq studies as dependent upon RpoS, Rrp1, or Rel_{Bbu} (Caimano et al.,
259 2015; Drecktrah et al., 2015; Grassmann et al., 2023), which are the three main *Bb* regulatory
260 programs active in the tick (Samuels et al., 2021). These additional genes highlight the necessity
261 of measuring transcription in the tick environment and suggest we uncovered gene expression
262 changes specific to the tick-stage of the *Bb* enzootic cycle. The nature and dynamics of these
263 changes provide insights into potential genetic determinants of *Bb* survival, proliferation, and
264 dissemination in the tick during transmission.
265
266 ***Bb* genes upregulated during feeding are found predominantly on plasmids**
267 *Bb* has a complex, highly fragmented genome (Barbour, 1988) (**Figure 3A**), including numerous
268 plasmids that are necessary during specific stages of the enzootic cycle (Schwartz et al., 2021)
269 suggesting they contain genes that are crucial for pathogen transmission and survival. In fact,
270 many genes found on the plasmids have been previously shown to alter expression upon
271 environmental changes or in different host environments (Iyer et al., 2015; Ojaimi et al., 2005;
272 Revel et al., 2002; Tokarz et al., 2004). Thus, we reasoned that many of the 192 DE *Bb* genes
273 that change expression from day 1 to any later feeding time point (**Table S4**) would reside on the
274 plasmids, and we examined their distribution throughout the genome. Consistent with these
275 previous reports, we found that most of the upregulated genes were located on the plasmids
276 (143/158; 90%), while fewer were found on the chromosome (15/158; 10%) (**Figure 3B**), which
277 is home to the majority of metabolic and other housekeeping genes. In contrast, the majority of
278 the downregulated genes were found on the chromosome (27/34, 79%) (**Figure 3C**).
279

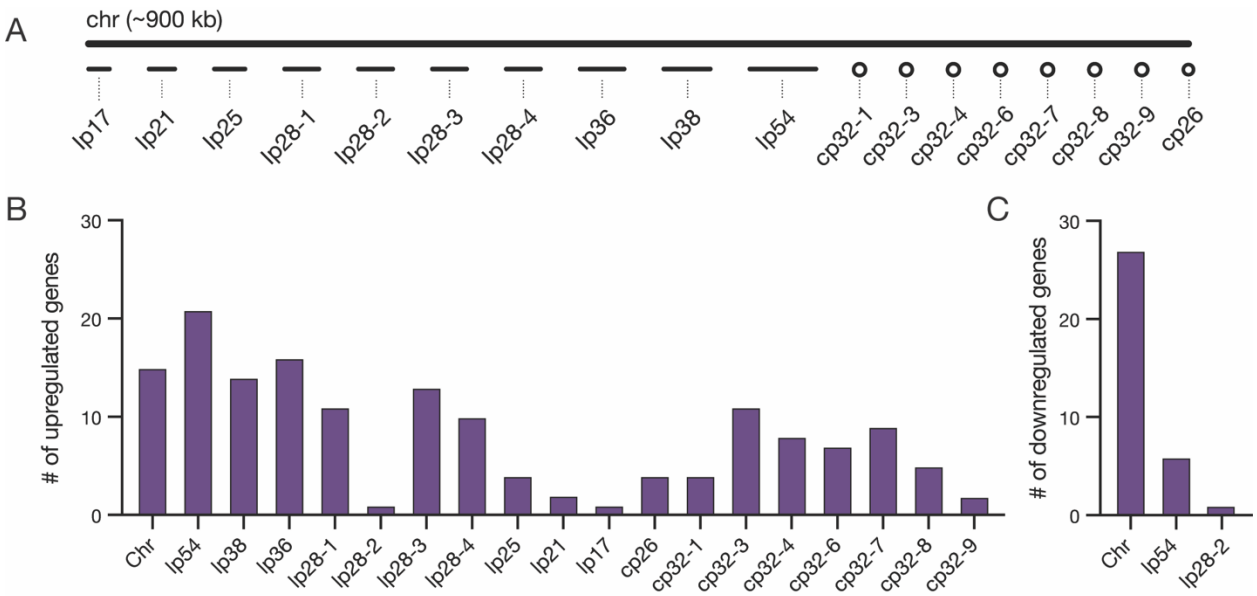

Figure 3. *Bb* genes upregulated during feeding are found predominantly on plasmids. (**A**) Schematic of the chromosome and plasmids in the *Bb* B31-S9 genome. Plasmid names denote whether the plasmid is linear (lp) or circular (cp) and the length of plasmids in kilobases (kb). For example, lp17 is a 17 kb linear plasmid. Genome is shown approximately to scale. (**B-C**) The number of genes from each chromosome or plasmid that increased (**B**) or decreased expression (**C**) twofold during feeding. Upregulated genes are distributed across plasmids, while downregulated genes are found on the chromosome and lp54.

280 Several plasmid-encoded genes that were longitudinally upregulated in our dataset have known
281 roles during the tick bloodmeal or in mammalian infection. Linear plasmid 54 (lp54),
282 which is an essential plasmid present in all *Bb* isolates (Casjens et al., 2012), contained the largest
283 number of upregulated genes. Many of the genes on lp54 are known to be regulated by RpoS
284 during feeding, including those encoding adhesins DbpA and DbpB, which are important for
285 infectivity in the host (Blevins et al., 2008). This set also included five members of a paralogous
286 family of outer surface lipoproteins BBA64, BBA65, BBA66, BBA71, and BBA73. BBA64 and
287 BBA66 are necessary for optimal transmission via the tick bite (Gilmore et al., 2010; Patton et al.,
288 2013). These findings indicate our dataset captures key *Bb* transcriptional responses known to
289 be important for survival inside the tick during a bloodmeal.
290
291 Many upregulated genes were also encoded by cp32 plasmid prophages. *Bb* strain B31-S9
292 harbors seven cp32 isoforms that are highly similar to each other (Casjens et al., 2012). When
293 cp32 prophages are induced, phage virions called ϕBB1 are produced (Eggers and Samuels,
294 1999). In addition to phage structural genes, cp32 contain loci that encode various families of
295 paralogous outer surface proteins (Stevenson et al., 2000). Amongst the cp32 genes that
296 increased over feeding were members of the RevA, Erp, and Mlp families, which are known to
297 increase expression during the bloodmeal (Gilmore et al., 2001). We also found several phage

genes that were upregulated, including those encoding proteins annotated as phage terminases on cp32-3, cp32-4, and cp32-7 (BBS45, BBR45, and BBO44). Some cp32 genes have been shown to change expression in response to the presence of blood (Tokarz et al., 2004), and as a part of the stringent response regulated by Rel_{Bbu} (Drecktrah et al., 2015), while BBD18 and RpoS regulate prophage production in the tick midgut after feeding (Wachter et al., 2023). Our data suggest that some prophage genes are upregulated over the course of tick feeding, raising the possibility that cp32 prophage are induced towards the end of feeding. Overall, our data support the long-held idea that the *Bb* plasmids, which house many genes encoding cell envelope proteins, proteins of unknown function, and prophage genes, play a critical role in the enzootic cycle during the key transition period of tick feeding.

_Bb_ genes encoding outer surface proteins are highly prevalent among upregulated genes

To gain a better overall sense of the types of genes that changed over feeding and the timing of those changes, we grouped DE genes into functional categories. Since a high proportion of plasmid genes encode lipoproteins within the unique protein-rich outer surface of *Bb*, genes of unknown function, and predicted prophage genes (Casjens et al., 2000; Fraser et al., 1997), we expected that many of the DE genes would fall into these categories. We classified the genes as related to either: cell envelope, bacteriophage, cell division, DNA replication and repair, chemotaxis and motility, metabolism, transporter proteins, transcription, translation, stress response, protein degradation, or unknown (Drecktrah et al., 2015) (see **Table S4**).

Of the genes that increased two-fold over feeding, the clear majority each day of feeding fell into two broad categories, cell envelope (55 of 158 total genes) and proteins of unknown function (69 of 158 total genes), with fewer genes related to metabolism, chemotaxis and motility, transporters, bacteriophage, cell division, and transcription (**Figure 4A**). In contrast to the upregulated genes, genes downregulated during feeding were more evenly distributed among the functional categories – including translation, protein degradation, transcription, and metabolism – consistent with many of them being located on the chromosome.

When looking at changes across these functional categories, the overrepresentation of cell envelope proteins was striking, while not unexpected. The *Bb* outer surface is covered with lipoproteins (**Figure 4B**), and these proteins are critical determinants in *Bb* interactions with the various environments encountered during the enzootic cycle (Kurokawa et al., 2020). We found

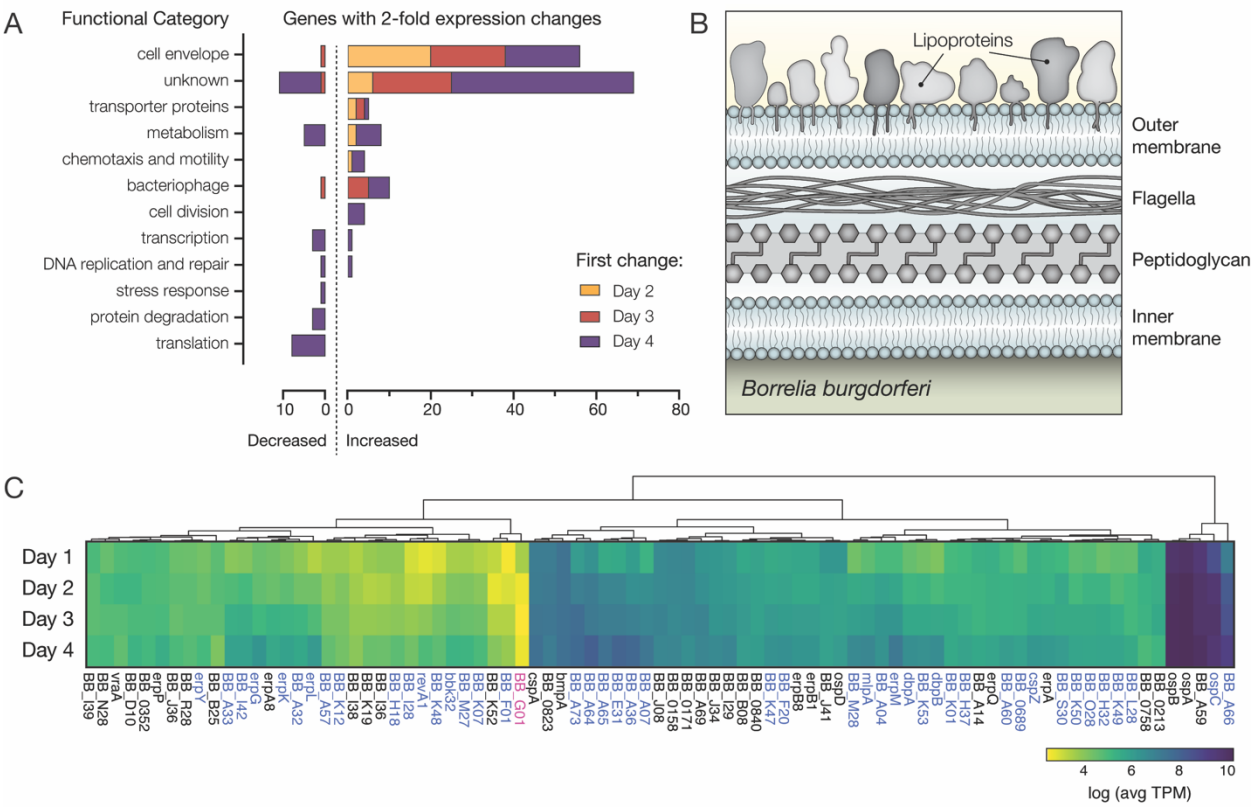

Figure 4. *Bb* genes encoding outer surface proteins are highly prevalent among upregulated genes. (**A**) The number of *Bb* genes that change over the course of tick feeding sorted into functional categories. Genes that first change 2 days after attachment are shown in yellow, 3 days after attachment in red, and 4 days after attachment in purple. A majority of upregulated genes fall into cell envelope and unknown categories. (**B**) Schematic of the outer membrane of *Bb* showing outer surface lipoproteins. Lipoproteins can also reside in the periplasmic space. (**C**) Heat map of expression levels of all genes encoding outer surface lipoproteins as average Transcripts Per Million (TPM) across the 4 days of tick feeding. Gene names highlighted in blue were two-fold upregulated and genes in pink two-fold downregulated over feeding (see **Figure 2**). A majority of genes encoding outer surface proteins increased in expression throughout feeding, while having different magnitudes of expression.

that more than half (46 of 83) of annotated outer surface lipoproteins (Dowdell et al., 2017; Iyer et al., 2015) changed expression two-fold over the time course (**Figure 4C**). These data suggested widespread changes may be occurring on the *Bb* outer surface during feeding.

To understand the functional implications of expression changes in a majority of outer surface lipoproteins, we also compared their relative expression. The magnitude of expression varied greatly, with *ospA*, *ospB*, *ospC*, and *bba59* being the most highly expressed outer surface protein transcripts. Many of the outer surface protein genes that we found increased expression over feeding were much less abundantly expressed (**Figure 4C** and **Table S5**). However, even the genes that appeared to have low expression in these population level measurements could play important roles in transmission if they are highly expressed in a small number of crucial cells, such as those that ultimately escape the midgut. While bulk RNA-seq cannot distinguish what is happening at the single cell level, our data suggest that during the bloodmeal, *Bb* are undergoing

344 a complex outer surface transformation driven by increases in transcription of a majority of the
345 genes encoding these lipoproteins.
346
347 **Identification of candidate tick interaction partners of *Bb* cells *ex vivo***
348 Our RNA-seq data suggested that the outer surface of *Bb* transforms over the course of feeding
349 as *Bb* are primed for transmission to a vertebrate host. At the same time, the tick midgut
350 environment is changing as the tick begins to digest its bloodmeal (Sonenshine and Anderson,
351 2014). Tick-*Bb* interactions are likely crucial at the beginning of the tick bloodmeal, as *Bb* adhere
352 to the tick gut epithelium before becoming motile and migrating out of the midgut and into the
353 salivary glands (Dunham-Ems et al., 2009). Some *Bb* outer surface proteins, such as BBE31 and
354 BBA52 play key roles in pathogen migration through interactions with the tick environment
355 (reviewed in Kurokawa et al., 2020). We wanted to explore the changing tick environment to
356 identify tick proteins with which *Bb* could interact throughout the tick bloodmeal. Since our *Bb*
357 enrichment process retained some tick material, we reasoned that tick proteins that interact with
358 *Bb* would be present in these samples.
359
360 To outline the changes occurring in the tick during feeding and to identify candidate *Bb*-interacting
361 tick proteins, we used mass spectrometry to survey the content of the tick material that was
362 enriched along with the *Bb* cells we sequenced at early and late stages during feeding. We purified
363 proteins from the α*Bb*-enriched fraction of crushed infected ticks one day after attachment and
364 four days after attachment in triplicate. As controls for each day, we also performed the *Bb*
365 enrichment process on lysate from uninfected ticks mixed with *in vitro* cultured *Bb* to help rule out
366 proteins that were not pulled down through *in vivo* tick-*Bb* interactions (**Figure 5A**). When
367 querying against the *Bb* and *I. scapularis* proteomes, we identified between 414 and 2240 protein
368 groups per sample replicate. The vast majority of all detected proteins were from ticks (2801/2858,
369 98%). To identify proteins of interest, we looked for those that were detected in at least two of
370 three replicates within infected ticks and had a mean average coverage twice that of uninfected
371 ticks mixed with cultured *Bb*. We found 256 proteins (251 from *I. scapularis* and 5 from *Bb*) that
372 were enriched with *Bb* from infected ticks one day after attachment and 226 proteins (220 from *I.*
373 *scapularis* and 6 from *Bb*) that were enriched with *Bb* from infected ticks four days after
374 attachment (**Table S6**). Of these proteins, only 27 (24 from *I. scapularis* and 3 from *Bb*) were
375 detectable on both days, suggesting the tick proteins present upon *Bb* enrichment change
376 dramatically over the course of feeding (**Figure 5A**). Amongst the small number of *Bb* proteins,
377 we identified OspC in the samples from day 4 after attachment but not day 1 after attachment,

378 confirming the expression change we saw in our RNA-seq. The distinct sets of tick proteins we
379 identified at each timepoint suggest dramatic changes occur in the *Bb*-infected tick midgut
380 environment during feeding that may alter the landscape of tick-*Bb* interactions.
381

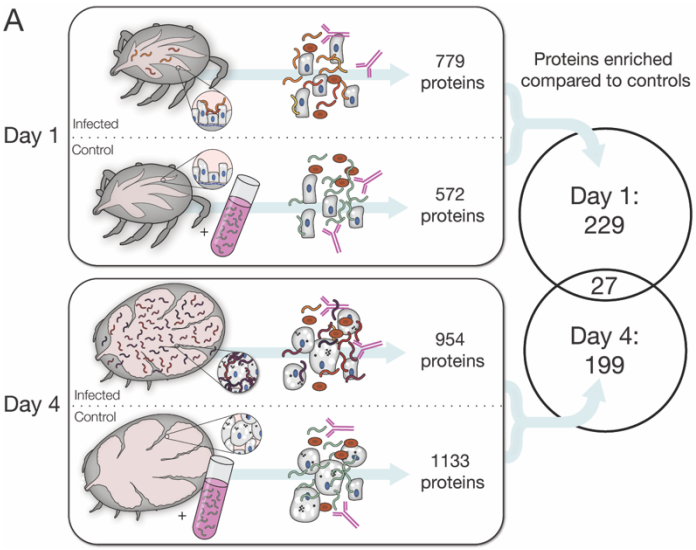

B Day 1: Extracellular matrix proteins

Uniprot ID	Description
B7QHE0	Laminin beta 1 chain, putative
B7Q8G4	Fibrillin-1, putative
B7PA51	Cuticle protein, putative
B7QKI7	Fibulin, putative
B7Q1H6	Laminin gamma-1 chain, putative
B7PDK2	Cuticular protein, putative
B7PYL8	Galectin
B7P6X9	Hemolectin, putative
B7PBS1	Cuticular protein, putative
B7P5P6	Uncharacterized protein

C Day 4: Membrane proteins

Uniprot ID	Description
B7PY45	Low-density lipoprotein receptor
B7PY43	Low-density lipoprotein receptor

Figure 5. Identification of candidate tick interaction partners of *Bb* cells *ex vivo*. (**A**) Schematic of experiment to determine candidate tick proteins interacting with *Bb* over the course of feeding. Ticks were collected 1 day after attachment and 4 days after attachment. Uninfected ticks at the same time points were mixed with cultured *Bb* as controls. *Bb* was enriched with α*Bb* antibody as in RNA-seq experiments and then subjected to mass spectrometry to identify tick proteins present in the samples. Venn diagram depicts the proteins enriched in day 1 and day 4 samples over controls in at least two of three replicates. Tick proteins that are enriched with *Bb* vary greatly over the course of feeding. (**B**) Tick proteins uniquely identified one day after attachment that are annotated as extracellular matrix (ECM) proteins. (**C**) Tick proteins uniquely identified four days after attachment that are annotated as low-density lipoprotein receptors. ECM and membrane proteins may be good candidates for *Bb*-interacting proteins.

382 Some of the proteins enriched with *Bb* from the tick may be good candidates for key *Bb*-interacting
383 partners during feeding, especially if they are localized to the surface of tick cells where they may
384 encounter *Bb*. The scarcity of both predicted and experimentally validated functions and
385 localizations for tick proteins makes it difficult to fully assess the potential for tick protein
386 interactions with extracellular *Bb*. Nevertheless, of the proteins found exclusively one day after
387 attachment, 10 were categorized as extracellular matrix proteins using the PANTHER gene
388 database (Thomas et al., 2022), and this category was statistically enriched (Fisher's exact test,
389 FDR=0.000093) (**Figure 5B** and **Table S7**). 30 additional proteins were annotated with a cellular
390 component as plasma membrane. Four days after attachment, we did not detect any annotated
391 extracellular matrix proteins; however, we identified 31 proteins that are likely to be found at the
392 membrane, including two proteins annotated as putative low-density lipoprotein receptors (**Figure**
393 **5C** and **Table S8**). These extracellular matrix and membrane proteins may be the most likely to
394 directly interact with *Bb* during this timeframe and are candidates for tick proteins important in the

395 *Bb* dissemination process. The proteins present in the changing tick environment may be key
396 determinants of pathogen transmission as *Bb* remodels its outer surface while preparing to
397 migrate through the tick to a new host.
398
399 **DISCUSSION**
400 Vector-borne pathogens must adapt to distinct environments as they are transmitted by
401 arthropods to colonize new bloodmeal hosts. The tick-borne Lyme disease pathogen *Bb*
402 undergoes transcriptional changes inside its vector over the course of a single bloodmeal that are
403 important for a number of key transmission events. For example, expression changes enable
404 survival in the feeding tick (He et al., 2011), facilitate transmission across several internal
405 compartments into the bloodmeal host (Kurokawa et al., 2020), and prime bacteria for successful
406 infection of the next host (Kasumba et al., 2016). Capturing these changes as they occur *in vivo*
407 has been challenging due to the low relative abundance of *Bb* material inside of the rapidly
408 growing, blood-filled tick. To date, many advances in our understanding of *Bb* expression during
409 transmission from tick to host have come from tracking changes in small subsets of genes during
410 tick feeding (Bykowski et al., 2007; Gilmore et al., 2001; Narasimhan et al., 2002), leveraging *Bb*
411 culture conditions that approximate environmental changes across its lifecycle (Ojaimi et al.,
412 2005; Revel et al., 2002; Tokarz et al., 2004), and defining transcriptional regulons outside of the
413 tick (Caimano et al., 2019, 2015; Drecktrah et al., 2015). Here, we developed an experimental
414 RNA-seq-based strategy to more directly and longitudinally profile gene expression for *Bb*
415 populations isolated from ticks over the course of a transmitting bloodmeal.
416
417 Our longitudinal collection of transcriptomes for *Bb* cells isolated from ticks serves as a resource
418 and starting point for delineating the functional determinants of *Bb* adaptation and transmission.
419 We focused our analysis on 192 genes that changed two-fold between day 1 and later days in
420 feeding. While these genes were highly concordant with those found in previous studies probing
421 transcriptional changes throughout the *Bb* enzootic cycle (Caimano et al., 2019, 2015; Drecktrah
422 et al., 2015; Grassmann et al., 2023; Iyer et al., 2015; Ojaimi et al., 2003; Revel et al., 2002), our
423 transcriptome profiles revealed changes in expression of 26 genes not observed in these previous
424 studies. These novel gene expression changes, like all of the 192 DE genes, were concentrated
425 in genes of unknown function and those encoding outer surface proteins. Although challenging to
426 address, efforts focused on uncovering the contribution of the genes of unknown function to the
427 *Bb* life cycle could be groundbreaking for understanding the unique aspects of tick-borne
428 transmission. Our data reveal more extensive expression changes for *Bb* outer surface proteins

429 than previously appreciated, with nine additional genes encoding cell envelope proteins
430 upregulated over feeding that were not found to change expression in the previous studies
431 examining unfed versus fed tick conditions or nymphs versus DMCs. The extensive changes in
432 genes encoding outer surface proteins suggest *Bb* is actively remodeling its outer coat to navigate
433 the dynamic tick environment during feeding, akin to wardrobe changes across seasons. These
434 outer surface changes may play roles in the persistence of *Bb* in the tick, cell adhesion, or in
435 immune evasion, either inside of the tick or later in the vertebrate host (Kenedy et al., 2012). It
436 has long been observed that molecular interactions between pathogens and the midgut of their
437 vectors are key determinants of transmission (Barillas-Mury et al., 2022). Modifications to the *Bb*
438 surface could facilitate different tick–pathogen interactions that are critical for its physical
439 movement through tick compartments.
440
441 More comprehensive knowledge about *Bb* outer surface proteins and their functional
442 consequences could lead to new avenues for curtailing the spread of Lyme disease. Protective
443 vaccines against vector-borne pathogens have often targeted surface proteins encoded by
444 pathogens (Kovacs-Simon et al., 2010). While previous Lyme disease vaccine efforts effectively
445 targeted the highly expressed *Bb* outer surface protein OspA (Steere et al., 1998), more targets
446 could increase the likelihood of a successful vaccine. Our study provides a catalog of new *Bb*
447 candidates that could be explored. In addition, our biochemical pull-downs using tick-isolated *Bb*
448 cells as bait unearthed a preliminary list of potential tick proteins that could be involved in tick–*Bb*
449 interactions. Blocking molecular interactions that are functionally critical for transmission could
450 also be explored as a therapeutic strategy (Barillas-Mury et al., 2022; Manning and Cantaert,
451 2019).
452
453 To identify the genes changing expression during tick feeding, we used an antibody targeting *Bb*
454 to overcome the low abundance of *Bb* in the tick. This method produced broad coverage of the
455 transcriptome over our time course, but there are caveats. While we confirmed that the hour-long
456 enrichment procedure does not cause significant gene expression changes in cultured *Bb*, this
457 may still influence gene expression in our *ex vivo* samples. The α*Bb* antibody, which targets OspA
458 and a number of other proteins, captured the vast majority, but not all, *Bb* from inside of the tick.
459 This loss may introduce some degree of bias. Further, a large number of day 4 reads mapping to
460 *P. fulva* suggests that this particular antibody may enrich other bacterial species. It is also
461 important to note that our method was unable to produce consistent expression data from *Bb* from
462 unfed ticks, limiting the full longitudinal scope of the study and potentially overlooking key changes

463 occurring in the first 24 hours of feeding. We predict this difficulty may be due to low numbers of
464 *Bb* in flat nymphs (de Silva and Fikrig, 1995) or the stress of the prolonged nutrient-deprived
465 period between tick feedings (Kung et al., 2013). The transcriptional landscape of unfed ticks may
466 be better probed through enrichment after RNA-seq library preparation such as TBDCapSeq
467 (Grassmann et al., 2023), or perhaps a combination of the two enrichment strategies. Despite
468 these caveats, this type of antibody-based enrichment strategy is a simple and flexible technique
469 that can probe gene expression from *Bb* from multiple timepoints in feeding ticks. With small
470 modifications, this protocol may be able to assist in facilitating sequencing of *Bb* or other *Borrelia*
471 species from other milieu or enrich other tick-borne bacterial species.
472
473 Our method has produced a transcriptomic resource providing critical insights into *Bb* population-
474 level changes during the vector stage of its lifecycle, which serves as a starting point for
475 understanding the primary drivers of tick-borne transmission. Strikingly few *Bb* cells out of the
476 total pathogen population in ticks are ultimately transmitted to the next host during feeding
477 (Dunham-Ems et al., 2009; Rego et al., 2014). There may be important molecular variations
478 across *Bb* cells within the population residing in the tick that contribute to these differential
479 outcomes including heterogeneously expressed proteins across cells within the feeding tick
480 midgut (Ohnishi et al., 2001). Genes that appear unaltered or show low expression levels across
481 the bulk population could still play an outsized role in infection for a minority of the cells, and
482 conducting transcriptomic analyses at the single-cell level will be key. Our work provides a
483 foundational methodology that can be leveraged to greatly improve the resolution of tick–microbe
484 studies. Technological advances stemming from this work will provide molecular may unearth
485 surprising mechanistic insights into the unique lifestyles of tick-borne pathogens.
486
487 **METHODS**
488 ***B. burgdorferi* culture**
489 *Bb* strain B31-S9 (Rego et al., 2011) was provided by Dr. Patricia Rosa (NIAID, NIH, RML) and
490 cultured in BSK II media at 35°C, 2.5% CO_2. B31-S9 was used for all RNA-seq and *Bb* enrichment
491 experiments. Wildtype *Bb* strain B31-A3, ospA1-mutants (ospA1) and ospA-restored *Bb*
492 (ospA$^+$B1) (Battisti et al., 2008) used in α*Bb* western blot were also provided by Dr. Rosa.
493
494 **Tick feeding experiments**
495 *I. scapularis* larvae were purchased from the Tick Lab at Oklahoma State University (OSU) for
496 RNA-seq experiments or provided by BEI Resources, a division of the Center for Disease Control,

497 for mass spectrometry experiments. Before and after feeding, ticks were maintained in glass jars
498 with a relative humidity of 95% (saturated solution of potassium nitrate) in a sealed incubator at
499 22°C with a light cycle of 16h/8h (light/dark). Animal experiments were conducted in accordance
500 with the approval of the Institutional Animal Care and Use Committee (IACUC) at UCSF, Project
501 Number AN183452. Ticks were fed on young (4–6-week-old) female C3H/HeJ mice acquired from
502 Jackson Laboratories. Mice were anesthetized with ketamine/xylazine before placement of ≤ 100
503 larval or ≤ 30 nymphal ticks. Replete larval ticks were placed in the incubator to molt before being
504 used as nymphs in experiments. Nymphal ticks were either pulled off isoflurane anesthetized mice
505 at various times during feeding (1-3 days after placement) or allowed to feed to repletion and
506 collected from mouse cages (4 days after placement).
507
508 **Western blot with α*Bb* antibody**
509 To determine whether the α*Bb* antibody targeted ospA, wildtype *Bb* (B31-A3), ospA1-mutants
510 (ospA1) and ospA-restored *Bb* (ospA^{+}B1) (Battisti et al., 2008) were cultured to approximately
511 5x10^{7} *Bb*/mL. 3 mLs of culture were centrifuged for 7 minutes at 8000 x g, washing twice with
512 PBS. Pelleted cells were lysed in 50 µL of water, and 25 µg of protein per sample were mixed
513 with 5X loading dye (0.25% Bromophenol Blue, 50% Glycerol, 10% Sodium Dodecyl Sulfate,
514 0.25M Tris-Cl pH 6.8, 10% B-Mercaptoethanol), run on a Mini-PROTEAN TGX 4-15% gel
515 (Biorad), and transferred using the Trans-Blot Turbo Transfer System (Biorad). After transfer, the
516 blot was blocked for 30 minutes at 4°C in TBST (Tris buffered saline with 0.1% tween) with 5%
517 milk, then treated with α*Bb* antibody (Invitrogen: PA1-73004; RRID: AB_1016668) diluted
518 1:10,000 for 1 hour at room temperature, followed by anti-rabbit HRP secondary antibody
519 (Advansta: R-05072-500; RRID: AB_10719218) diluted 1:5,000 for 45 minutes at room
520 temperature with 3 short PBST washes between each step. Blots were exposed using Clarity
521 Western ECL Substrate (Biorad) and imaged using the Azure C400 imaging system (Azure
522 Biosystems). This experiment was repeated three times.
523
524 **Enrichment of *Bb* from feeding ticks**
525 To sequence RNA from *Bb* from feeding ticks, *Bb* were enriched to increase the ratio of *Bb* to tick
526 material. Larval ticks were fed to repletion on three mice that were infected with *Bb* through
527 intraperitoneal and subcutaneous injection with 10^{4} total *Bb*. Approximately five months later, the
528 molted nymphal ticks were fed on eight mice, which were housed individually during the feeding.
529 We estimated that 83% of the ticks were infected with *Bb* by crushing 12 unfed nymphs in BSK II
530 media and checking for viable *Bb* days later. Ticks were pulled from all mice and pooled into four

531 biological replicates 1 day after placement (14 ticks per replicate), 2 days after placement (12
532 ticks per replicate), and 3 days after placement (6 ticks per replicate) and collected from cages 4
533 days after placement (7 ticks per replicate). Shortly after collection, ticks were washed with water
534 and placed in a 2 mL glass dounce grinder (Kimble) in 500 µL of phosphate-buffered saline (PBS).
535 Ticks were homogenized first with the large clearance pestle and then the small clearance pestle.
536 The homogenate was transferred to a 1.5 mL Eppendorf tube and 500 µL of PBS was added to
537 total 1 mL. At this stage, 50 µL of homogenate was removed as an input sample and mixed with
538 500 µL of TRIzol (Invitrogen) for RNA extraction. 2 µL of α*Bb* antibody (Invitrogen: PA1-73004;
539 RRID: AB_1016668) was added to the homogenate, which was then placed on a nutator at 4°C
540 for 30 minutes. During incubation, 50 µL of Dynabeads Protein G (Invitrogen) per sample were
541 washed twice in PBS. After incubation with the antibody, the homogenate and antibody mixture
542 were added to the beads. This mixture was placed on a nutator at 4°C for 30 minutes. Tubes were
543 then placed on a magnet to secure beads, and the homogenate was removed and saved to create
544 depleted samples. The depleted homogenate was centrifuged at 8,000 x g for 7 minutes, 900 µL
545 of supernatant was removed, and 500 µL of TRIzol was added to the pellet to create depleted
546 samples. The beads were washed twice with 1 mL of PBS, resuspending the beads each time.
547 The second wash was removed and 500 µL of TRIzol was added to the beads to create enriched
548 samples. RNA was extracted from all input, enriched, and depleted samples using the Zymo
549 Direct-zol RNA Microprep Kit with on-column DNase treatment (Zymo Research). The step-by-
550 step *Bb* enrichment protocol is available at: dx.doi.org/10.17504/protocols.io.36wgqjrbovk5/v1.
551
552 **Enrichment of *Bb* from culture**
553 To test whether the *Bb* enrichment process altered gene expression levels, we performed the
554 enrichment protocol on cultured *Bb*. Tubes of *Bb* in BSK II media were grown to $9x10^4$ *Bb*/mL at
555 35°C. 1 mL of culture was spun down at 8,000 x g for 7 minutes, media was removed, *Bb* were
556 washed in 1mL of PBS and spun again. Pelleted *Bb* were resuspended in 1 mL of fresh PBS.
557 These samples were used as starting homogenate for the *Bb* enrichment protocol and input,
558 enriched, and depleted fractions were collected as above. RNA-seq libraries from these samples
559 were prepared and sequenced as below.
560
561 **RNA-seq library preparation and sequencing**
562 To make RNA-seq libraries from enriched *Bb* RNA, 50 ng of total RNA was used as input into the
563 NEBNext Ultra II Directional RNA Library Prep Kit for Illumina (New England BioLabs). Libraries
564 were prepared following the manufacturer's protocol for use of the kit with purified mRNA or rRNA-

565 depleted RNA, despite starting with total RNA. Libraries were barcoded using NEBNext Multiplex
566 Oligos for Illumina Dual Index (New England BioLabs).
567
568 To deplete reads from the libraries that were from tick, *Bb*, or mouse rRNA, we used Depletion of
569 Abundant Sequences by Hybridization (DASH) (Gu et al., 2016), which targets Cas9 to unwanted
570 reads in RNA-seq libraries using custom dual-guide RNAs (dgRNAs). The dgRNAs targeted short
571 sequences within tick rRNA, mouse rRNA, and *Bb* rRNA that were designed using DASHit
572 software (Dynerman et al., 2020). We ordered crRNA oligos (**Table S9**) that targeted these
573 sequences (Ring et al., 2022). To transcribe the dgRNAs, we followed the protocol for *In Vitro*
574 Transcription for dgRNA V2 (Lyden et al., 2019b) as follows. Both tracrRNA and pooled crRNA
575 DNA templates were annealed to equimolar amounts of T7 primer by heating to 95°C for 2
576 minutes and slowly cooling to room temperature. Annealed templates were used in 1 mL *in vitro*
577 transcription reactions with: 120 µL10X T7 buffer (400 mM Tris pH 7.9, 200 mM MgCl2, 50 mM
578 DTT, 20 mM spermidine (Sigma)), 100 µL of T7 enzyme (custom prepped enzyme from E.
579 Crawford, diluted 1:100 in T7 buffer, final concentration: 100 µg/mL), 300 µl NTPs (25 mM each,
580 Thermo Fisher Scientific), 4 µg of annealed crRNA template or 8 µg of annealed tracrRNA
581 template, and water to 1 mL. *In vitro* transcription was performed for 2 hours at 37°C. Reactions
582 were purified twice with the Zymo RNA Clean & Concentrator-5 Kit (Zymo Research). To form the
583 dgRNA complex for DASH, crRNA and tracrRNAs were diluted to 80 µM, mixed in equimolar
584 amounts and annealed by heating to 95ºC for 30 seconds and cooling slowly to room temperature.

585 After transcription of dgRNAs, we performed DASH Protocol Version 4 (Lyden et al., 2019a) on
586 each library individually as follows. Cas9 and transcribed dgRNAs were prepped by mixing: 2.5
587 µL 10X Cas9 buffer, 5 µL 20 µM Cas9 (New England BioLabs), and 5 µL of 40 µM transcribed
588 dgRNAs. The mixture was incubated at 37°C for 5 minutes before 7.5 µL of RNA-seq library (2.8
589 nM) was added. The mixture was incubated at 37°C for 1 hour and then purified with Zymo DNA
590 Clean & Concentrator-5 (Zymo Research) following the PCR product protocol and eluting DNA
591 into 10.5 µL of water. During cleanup, Cas9 was again mixed with buffer and dgRNAs and
592 incubated at 37°C for 5 minutes. Following cleanup, eluted DNA was added to the second Cas9-
593 dgRNA mixture and incubated at 37°C for 1 hour for a second time. Then, 1 µL of proteinase K
594 (New England Biolabs) was added, and the mixture was incubated at 50°C for 15 min. The
595 libraries were then purified with 0.9X volume of sparQ PureMag Beads (QuantaBio) following the
596 standard protocol, eluting in 24 µL of water. rRNA-depleted RNA-seq libraries were then amplified
597 in a BioRad CFX96 using the Kapa HiFi Real-Time Amplification Kit (Roche) in a 50 µL reaction

598 with 25 µL master mix, 23 µL of the DASHed library pool, and 2 µL of a 25 µM mix of Illumina P5
599 (5'-AATGATACGGCGACCACCGAGATCT) and P7 (5'- CAAGCAGAAGACGGCATACGAGAT)
600 primers. The qPCR program for amplification was as follows: 98°C for 45 sec (1 cycle), (98°C for
601 15 sec, 63°C for 30 sec, 72°C for 45 sec, plate read, 72°C for 20 sec) for 10 cycles (day 3 and
602 day 4 samples) or 11 cycles (day 1 and day 2 samples). The libraries were removed from cycling
603 conditions before leaving the exponential phase of amplification and then purified with 0.9X
604 volume of sparQ PureMag Beads according to the standard protocol.

605 Following DASH, RNA-seq libraries were sequenced on an Illumina NovaSeq S2 (2 lanes) with
606 paired-end 100 base pair reads. Libraries from *in vitro* cultured control experiment were
607 sequenced on an Illumina NextSeq with paired-end 75 base pair reads. FASTQ files and raw *Bb*
608 read counts for *in vitro* control experiment (GSE217146) and *ex vivo* experiment (GSE216261)
609 have been deposited in NCBI's Gene Expression Omnibus (Edgar et al., 2002) under SuperSeries
610 accession number GSE217236.

611 **RNA-seq data analysis**

612 ***DASH***

613 To measure the success of our rRNA depletion through DASH, we used DASHit software
614 (Dynerman et al., 2020) to determine the percentage of reads that would be DASHable by our
615 guide RNAs (Ring et al., 2022). For pre-DASH data, we sequenced the input of each of our RNA-
616 seq libraries before performing DASH on a MiSeq V2 Micro (Illumina). We tested DASHability on
617 a random subset of 200,000 paired-end reads chosen by seqtk (https://github.com/lh3/seqtk) from
618 each pre- and post-DASH library. Paired t test comparing DASHable reads before and after DASH
619 was performed using GraphPad Prism v9.5.1.
620

621 ***Differential expression analysis***

622 To map our RNA-seq data to *Bb*, we wanted to optimize for mapping reads that came from the
623 many paralogous gene families found across the plasmids of the genome. We used the
624 pseudoalignment tool Salmon v1.2.1 (Patro et al., 2017), which is used to accurately map reads
625 coming from different isoforms of the same gene, for this reason. While using Salmon to map to
626 CDS sequences may improve mapping to paralogous genes, it may also have a tradeoff of
627 reduced mapping of reads that fall on the ends of genes that reside in operons. Nevertheless, all
628 samples should be similarly affected, and any undercounting should not change differential
629 expression results. Reads were first trimmed of bases with quality scores less than 20 using
630 Cutadapt (Martin, 2011) via Trim Galore v0.6.5 (https://github.com/FelixKrueger/TrimGalore).

631 Reads were mapped to *Bb* CDS sequences as a reference transcriptome: NCBI Genbank
632 GCA_000008685.2 ASM868v2 (with plasmids lp5, cp9, and lp56 removed as they are not present
633 in B31-S9) using Salmon with the following parameters: --validateMappings --seqBias --
634 gcBias. Before mapping, the transcriptome was indexed using the Salmon index command with
635 the whole genome as decoys and the parameter --keepDuplicates to keep all duplicate genes.
636
637 Read counts from Salmon were used as input into DESeq2 v1.24.0 (Love et al., 2014) for
638 differential expression analysis in R version 3.6.1. DESeq2 function PlotPCA() was used to create
639 a PCA plot from read counts after running the varianceStabilizingTransformation() function. For
640 differential expression analysis between days, a DESeq object was created from count data using
641 the DESeq() function. The lfcShrink() function with the apeglm method (Zhu et al., 2018) was
642 used to calculate fold changes between days. DESeq2 uses a Benjamini-Hochberg multiple
643 testing correction, and we focused the majority of our analysis on genes that had an adjusted p-
644 value < 0.05 and used an additional cutoff requiring genes to change two-fold between conditions.
645 Code used for differential expression analysis is available at: https://github.com/annesapiro/Bb-
646 tick-feeding.
647
648 ***Mapping to other species***
649 To determine the source of non-*Bb* reads in our RNA-seq libraries, trimmed reads were mapped
650 to tick and mouse genomes using STAR v2.7.3a (Dobin et al., 2012). The *I. scapularis* ISE6
651 genome (RefSeq assembly GCF_002892825.2, ISE6_asm2.2_dedeplicated) (Miller et al., 2018)
652 was indexed using STAR run mode genomeGenerate with option --genomeChrBinNbits 18. The
653 *Mus musculus* genome GRCm39 (RefSeq assembly GCF_000001635.27) was indexed using
654 STAR run mode genomeGenerate with basic options. Reads were mapped using STAR to each
655 genome using basic options. The percentage of reads that mapped to these genomes was
656 determined by adding the percentage of uniquely mapped reads, reads mapped to multiple loci,
657 and reads mapped to too many loci. To identify the potential source of reads that did not map to
658 tick, mouse, or *Bb* in day 4 samples, one million reads from day 1 and day 4 libraries were used
659 as input into CZ ID (Kalantar et al., 2020), which determined that a large number of reads mapped
660 to bacterial species *Pseudomonas fulva*. Full RNA-seq libraries were then mapped to the *P. fulva*
661 genome (NCBI GenBank GCF_001186195.1 ASM118619v1), using the standard options of
662 Bowtie2 (Langmead and Salzberg, 2012) to calculate the overall alignment rate.
663
664 ***Comparisons to other studies***

665 Genes identified in previous studies were compared to time course expression changes. Here we
666 considered RpoS-regulated genes as those found in Grassmann et al. 2023 that were upregulated
667 by RpoS in both fed nymphs and DMCs and those upregulated by RpoS only during tick
668 transmission (Grassmann et al. Supplemental Tables 5 and 6). RpoS did not suppress the
669 expression of any genes in fed nymphs in the study. Genes up- and down-regulated by RpoS in
670 DMCs only (Grassmann et al. Supplemental Tables 7 and 8) are noted in **Table S3** and **Table S4**
671 for reference along with genes found to be regulated by RpoS in DMCs in Caimano et al. 2019
672 (Tables 2 and 3), which were used for RpoS comparisons in previous versions of this study. Rrp1
673 up- and down-regulated genes were those identified *in vitro* in Caimano et al. 2015, Table S2.
674 Rel_{Bbu} up- and down-regulated genes were examined by Drecktrah et al. 2015 in three different
675 *in vitro* conditions: starvation (Tables S6 and S9), recovery (Tables S7 and S10), and stationary
676 phase (Tables S5 and S8). For simplicity, we considered genes as Rel_{Bbu}-regulated if they were
677 up- or down-regulated in one or more of these conditions (**Tables S3** and **S4**). One gene was
678 regulated in opposing directions across conditions and is noted in our tables as "both" and was
679 excluded from the comparison analysis. Genes changing between "unfed tick" and "fed tick"
680 culture conditions in Revel et al. 2002 were those in Table 3. Genes from Ojaimi et al. 2003 Table
681 4 with increased expression *in vitro* at 35°C relative to 25°C were considered higher in "fed tick"
682 while those in Ojaimi et al. 2003 Table 5 with increased expression at 25°C relative to 35°C were
683 considered higher in "unfed tick." Genes more highly expressed in nymphs than DMCs from Iyer
684 et al. 2015 were found in Table S4, and genes more highly expressed in DMCs than nymphs were
685 found in Table S8. Genes differentially expressed between nymphs and DMCs in Grassmann et
686 al. 2023 were determined from the DESeq2 comparison between WT DMC vs Fed Nymphs found
687 in Supplemental Table 3, in accordance with their cutoffs of at least a three-fold difference and q-
688 value < 0.05. As many of these studies used different strains of *Bb* and different genome
689 annotations, some genes were not examined here as they were not present in the B31-S9 strain
690 used here.
691
692 ***Gene classification***
693 To classify genes into functional groups, functional categories were sourced from (Drecktrah et
694 al., 2015) where available. Other gene functions were sourced from (Fraser et al., 1997). Genes
695 found within the co-transcribed "late" bacteriophage operon (Zhang and Marconi, 2005) were
696 considered "bacteriophage" even if their function is unknown. Outer surface proteins were those
697 found in Dowdell et al., 2017 plus additional outer surface proteins listed in Iyer et al., 2015 that
698 were also found in Dowdell et al. 2017 Supporting Table S2 categories SpII and SpI as evidence

699 of outer surface localization. Outer surface and periplasmic lipoproteins were classified as "cell
700 envelope" in the absence of other classifications. Gene family information from (Casjens et al.,
701 2000) was considered to aid in classification. **Table S4** contains the classification source for each
702 gene.
703
704 **RT-qPCR measuring *Bb* enrichment**
705 To test the efficacy of the *Bb* enrichment protocol, RT-qPCR was used to quantify *Bb flaB* and *I.*
706 *scapularis gapdh* transcript levels in enriched and depleted fractions. cDNA was synthesized from
707 8 µL of RNA extracted from *Bb* enrichment samples and their matched depleted samples from
708 day 2, day 3, and day 4 post-attachment using the qScript cDNA Synthesis Kit (Quantabio). cDNA
709 was diluted 2X before use in qPCR. To measure *flaB* copies, standards of known concentration
710 were created from purified PCR products. These standards were made from PCR with primers
711 with the following sequences: 5'-CACATATTCAGATGCAGACAGAGGTTCTA and 5'-
712 GAAGGTGCTGTAGCAGGTGCTGGCTGT. A dilution series with ten-fold dilutions between 10^6
713 copies and 10^1 copies of this PCR template was run alongside enriched and depleted samples.
714 qPCR was performed using Taqman Universal PCR Master Mix (Applied Biosystems). The
715 primers used to amplify *flaB* were: 5'- TCTTTTCTCTGGTGAGGGAGCT and 5'-
716 TCCTTCCTGTTGAACACCCTCT (used at 900 nM) and the probe was /56-
717 FAM/AAACTGCTCAGGCTGCACCGGTTC/36-TAMSp (used at 250 nM). For tick *gapdh* RT-
718 qPCR, the cDNA samples were diluted an additional 2X. Standards of known concentration were
719 created using the qPCR primer sequences: 5'-TTCATTGGAGACACCCACAG and 5'-
720 CGTTGTCGTACCACGAGATAA (used at 900 nM). qPCR was performed using PowerUp SYBR
721 Green Master Mix (Applied Biosystems). For both *flaB* and *gapdh*, the number of copies in each
722 sample was calculated based on the standards of known concentration. Three technical replicates
723 were averaged from each of four biological replicates at each time point tested. We totaled the
724 number of copies in each matched enriched and depleted fraction to calculate the percentage of
725 *flaB* or *gapdh* that was found in either sample. All qPCR was performed on the QuantStudio3
726 Real-Time PCR System (Applied Biosystems). Paired t tests were performed using GraphPad
727 Prism v9.5.1.
728
729 **Immunofluorescence microscopy**
730 To test whether the α*Bb* antibody recognized *Bb* inside of the tick, ticks at each day of feeding
731 were crushed in 50 µL of PBS. 10 µL of lysate was spotted onto slides and allowed to air dry
732 before slides were heated briefly three times over a flame. Heat fixed slides were then treated

733 with acetone for one hour. Slides were incubated with α*Bb* primary antibody (1:100 diluted in PBS
734 + 0.75% BSA) for 30 minutes at 37°C in a humid chamber. A control without primary antibody
735 was also used for each day. Slides were washed once in PBS for 15 minutes at room temperature,
736 then rinsed in distilled water and air dried. Anti-rabbit IgG Alexa 488 (Invitrogen: A-11008; RRID:
737 AB_143165) diluted 1:100 in PBS + 0.75% BSA was added for 30 minutes at 37°C in a humid
738 slide chamber. Slides were washed in PBS for 15 minutes at room temperature three times,
739 adding 1:100 Propidium Iodide (Invitrogen) during the second wash. Slides were then rinsed with
740 distilled water and air dried before the addition of mounting media (Fluoromount-G,
741 SouthernBiotech) and cover slips. Fluorescence imaging was performed on a Nikon Ti2 inverted
742 microscope for widefield epifluorescence using a 100X/1.40 objective. Images were captured with
743 NIS-Elements AR View 5.20 and then processed with ImageJ software (Schneider et al., 2012).
744 No strong florescence signal was observed on the control slides without primary antibody.
745
746 **Mass spectrometry of *Bb*-enriched samples**
747 To identify which tick proteins were found in samples after *Bb* enrichment across feeding, both
748 uninfected and infected ticks were fed on mice. Three biological replicates of uninfected ticks one
749 day after attachment (11 ticks per replicate), infected ticks one day after attachment (27 ticks per
750 replicate), uninfected ticks four days after attachment (8 ticks per replicate), and infected ticks
751 four days after attachment (16 ticks per replicate) were collected. Before α*Bb* enrichment, the
752 uninfected tick samples were mixed with *Bb* grown in culture that was washed with PBS (3 x10^4
753 *Bb* one day after attachment and 3x10^6 *Bb* four days after attachment) and mixed lysates were
754 rotated at room temperature for 30 minutes. Infected tick samples underwent the *Bb* enrichment
755 process immediately. The enrichment process followed the same protocol used for RNA-seq.
756 Sample volumes were increased to 1 mL as needed, and then 2 µL of α*Bb* antibody (Invitrogen:
757 PA1-73004; RRID: AB_1016668) was added, and samples were rotated at 4°C for 30 minutes.
758 50 µL of Dynabeads Protein G per sample were washed in PBS during this incubation and added
759 to the lysates, which were rotated at 4°C for 30 minutes. The beads were washed twice with 1 mL
760 of PBS, and then placed into 50 µL of lysis buffer (iST LYSE, PreOmics). Samples were boiled at
761 95°C for 5 minutes, and lysates were removed from beads and frozen for mass spectrometry
762 preparation.
763
764 For mass spectrometry, a nanoElute was attached in line to a timsTOF Pro equipped with a
765 CaptiveSpray Source (Bruker). Chromatography was conducted at 40°C through a 25 cm
766 reversed-phase C18 column (PepSep) at a constant flowrate of 0.5 µL min−1. Mobile phase A

767 was 98/2/0.1% water/MeCN/formic acid (v/v/v) and phase B was MeCN with 0.1% formic acid
768 (v/v). During a 108 min method, peptides were separated by a 3-step linear gradient (5% to 30%
769 B over 90 min, 30% to 35% B over 10 min, 35% to 95% B over 4 min) followed by a 4 min isocratic
770 flush at 95% for 4 min before washing and a return to low organic conditions. Experiments were
771 run as data-dependent acquisitions with ion mobility activated in PASEF mode. MS and MS/MS
772 spectra were collected with m/z 100 to 1700 and ions with z = +1 were excluded.
773
774 Raw data files were searched using PEAKS Online Xpro 1.6 (Bioinformatics Solutions Inc.). The
775 precursor mass error tolerance and fragment mass error tolerance were set to 20 ppm and 0.03
776 respectively. The trypsin digest mode was set to semi-specific and missed cleavages was set to
777 2. The *I. scapularis* reference proteome (Proteome ID UP000001555, taxon 6945) and *Bb*
778 reference proteome (Proteome ID UP000001807, strain ATCC 35210/B31) was downloaded from
779 Uniprot, totaling 21,774 entries. The *I. scapularis* proteome was the primary search reference and
780 the *Bb* was used as a secondary to identify any bacterial proteins present. Carbamidomethylation
781 was selected as a fixed modification. Oxidation (M) and Deamidation (NQ) was selected as a
782 variable modification.
783
784 Experiments were performed in biological triplicate, with samples being a single run on the
785 instrument. Proteins present in a database search (−10 log(p-value) ≥ 20, 1% peptide and protein
786 FDR) were subjected to the following filtration process. Proteins were filtered to include only those
787 found in 2 out of 3 biological replicates, within each respective day (one or four days after
788 attachment). The mean area of proteins found in uninfected and infected samples was calculated.
789 Proteins with missing values (i.e. not identified in a sample) were set to 1. The ratio of mean area
790 for each protein was calculated as infected/uninfected, and enriched proteins were identified by
791 having an infected to uninfected ratio greater than 2 within their respective feeding day (one or
792 four days after attachment).
793
794 To classify the identified proteins into functional groups, a PANTHER Overrepresentation Test
795 (released 07/12/2022) was used (Mi et al., 2019) with PANTHER version 17.0 (released
796 02/22/2022) (Thomas et al., 2022). All *I. scapularis* genes in the database were used as the
797 reference list to and all proteins enriched on each day were analyzed for their PANTHER Protein
798 Class. The test type used was Fisher's Exact, calculating a false discovery rate as the correction.
799

Raw data files and searched datasets are available on the Mass Spectrometry Interactive Virtual Environment (MassIVE), a full member of the Proteome Xchange consortium under the identifier: MSV000090560.

DATA AVAILABILITY

For sequencing data, FASTQ files and raw *Bb* read counts for *in vitro* control experiment (GSE217146) and *ex vivo* experiment (GSE216261) have been deposited in NCBI's GEO database under SuperSeries accession number GSE217236. For mass spectrometry data, raw data files and searched datasets are available on the Mass Spectrometry Interactive Virtual Environment (MassIVE) under the identifier: MSV000090560. Code used for data analysis is available at: https://github.com/annesapiro/Bb-tick-feeding.

SUPPLEMENTAL TABLES

Table S1. Overview of mapping statistics from 16 *Bb* sequencing samples.

Table S2. Differential expression analysis results between *in vitro* cultured *Bb* before and after *Bb* enrichment.

Table S3. Transcriptome-wide differential expression analysis results from *Bb* across tick feeding timepoints.

Table S4. Two-fold differentially expressed *Bb* genes from across tick feeding timepoints.

Table S5. Transcripts per million (TPM) for all *Bb* genes across feeding timepoints.

Table S6. Mass spectrometry analysis for *Bb*-enriched samples.

Table S7. Annotation and GO term enrichment for tick proteins enriched on feeding day 1.

Table S8. Annotation and GO term enrichment for tick proteins enriched on feeding day 4.

Table S9. crRNAs targeting tick, mouse, and *Bb* rRNA sequences used in DASH.

ACKNOWLEDGMENTS

We are grateful to all members of the Chou lab for their feedback throughout the project, specifically to Fauna Yarza and Patrick Rockefeller Grimes for assistance with tick feeding and Ethel Ethel Enoex-Godonoo for administrative assistance. We thank Amy Lyden and Emily Crawford for assistance with and reagents for DASH along with Olga Botvinnik and The Chan Zuckerberg Biohub sequencing team for their input and sequencing assistance. We thank Patricia Rosa, Jenny Wachter, Scott Samuels, and Meghan Lybecker for their feedback on the project. We also thank William Hatleberg for assistance with figure schematics. This work was funded by: a Life Sciences Research Foundation fellowship from the SVCF-Wave Fund to Anne Sapiro, a

Beckman Young Investigator award from the Arnold and Mabel Beckman Foundation to Balyn Zaro, grants from CZ Biohub, the Pew Biomedical Research Foundation, and NIH funding 1R01AI132851 to Seemay Chou, and NIH INBRE funding P20GM103474 to Patrick Secor and Margie Kinnersley.

COMPETING INTERESTS

Seemay Chou is president and CEO of Arcadia Biosciences.

REFERENCES

Barbour AG. 1988. Plasmid analysis of *Borrelia burgdorferi*, the Lyme disease agent. *J Clin Microbiol* 26:475–478. doi:10.1128/jcm.26.3.475-478.1988

Barillas-Mury C, Ribeiro JMC, Valenzuela JG. 2022. Understanding pathogen survival and transmission by arthropod vectors to prevent human disease. *Science* 377:eabc2757. doi:10.1126/science.abc2757

Battisti JM, Bono JL, Rosa PA, Schrumpf ME, Schwan TG, Policastro PF. 2008. Outer Surface Protein A Protects Lyme Disease Spirochetes from Acquired Host Immunity in the Tick Vector. *Infect Immun* 76:5228–5237. doi:10.1128/iai.00410-08

Blevins JS, Hagman KE, Norgard MV. 2008. Assessment of decorin-binding protein A to the infectivity of *Borrelia burgdorferi* in the murine models of needle and tick infection. *Bmc Microbiol* 8:82. doi:10.1186/1471-2180-8-82

Bykowski T, Woodman ME, Cooley AE, Brissette CA, Brade V, Wallich R, Kraiczy P, Stevenson B. 2007. Coordinated Expression of *Borrelia burgdorferi* Complement Regulator-Acquiring Surface Proteins during the Lyme Disease Spirochete's Mammal-Tick Infection Cycle. *Infect Immun* 75:4227–4236. doi:10.1128/iai.00604-07

Caimano MJ, Dunham-Ems S, Allard AM, Cassera MB, Kenedy M, Radolf JD. 2015. Cyclic di-GMP Modulates Gene Expression in Lyme Disease Spirochetes at the Tick-Mammal Interface To Promote Spirochete Survival during the Blood Meal and Tick-to-Mammal Transmission. *Infect Immun* 83:3043–3060. doi:10.1128/iai.00315-15

Caimano MJ, Groshong AM, Belperron A, Mao J, Hawley KL, Luthra A, Graham DE, Earnhart CG, Marconi RT, Bockenstedt LK, Blevins JS, Radolf JD. 2019. The RpoS Gatekeeper in *Borrelia burgdorferi*: An Invariant Regulatory Scheme That Promotes Spirochete Persistence in Reservoir Hosts and Niche Diversity. *Front Microbiol* 10:1923. doi:10.3389/fmicb.2019.01923

Casjens S, Palmer N, Van Vugt R, Huang WM, Stevenson B, Rosa P, Lathigra R, Sutton G, Peterson J, Dodson RJ, Haft D, Hickey E, Gwinn M, White O, Fraser CM. 2000. A bacterial genome in flux: the twelve linear and nine circular extrachromosomal DNAs in an infectious

870 isolate of the Lyme disease spirochete *Borrelia burgdorferi*. *Mol Microbiol* 35:490–516.
871 doi:10.1046/j.1365-2958.2000.01698.x

872 Casjens SR, Mongodin EF, Qiu W-G, Luft BJ, Schutzer SE, Gilcrease EB, Huang WM,
873 Vujadinovic M, Aron JK, Vargas LC, Freeman S, Radune D, Weidman JF, Dimitrov GI,
874 Khouri HM, Sosa JE, Halpin RA, Dunn JJ, Fraser CM. 2012. Genome Stability of Lyme
875 Disease Spirochetes: Comparative Genomics of *Borrelia burgdorferi* Plasmids. *Plos One*
876 7:e33280. doi:10.1371/journal.pone.0033280

877 de Silva AM, Fikrig E. 1995. Growth and Migration of *Borrelia burgdorferi* in *Ixodes* Ticks during
878 Blood Feeding. *Am J Tropical Medicine Hyg* 53:397–404. doi:10.4269/ajtmh.1995.53.397

879 Dobin A, Davis CA, Schlesinger F, Drenkow J, Zaleski C, Jha S, Batut P, Chaisson M, Gingeras
880 TR. 2012. STAR: ultrafast universal RNA-seq aligner. *Bioinform Oxf Engl* 29:15–21.
881 doi:10.1093/bioinformatics/bts635

882 Dowdell AS, Murphy MD, Azodi C, Swanson SK, Florens L, Chen S, Zückert WR. 2017.
883 Comprehensive Spatial Analysis of the *Borrelia burgdorferi* Lipoproteome Reveals a
884 Compartmentalization Bias toward the Bacterial Surface. *J Bacteriol* 199:e00658-16.
885 doi:10.1128/jb.00658-16

886 Drecktrah D, Lybecker M, Popitsch N, Rescheneder P, Hall LS, Samuels DS. 2015. The
887 *Borrelia burgdorferi* RelA/SpoT Homolog and Stringent Response Regulate Survival in the
888 Tick Vector and Global Gene Expression during Starvation. *Plos Pathog* 11:e1005160.
889 doi:10.1371/journal.ppat.1005160

890 Dunham-Ems SM, Caimano MJ, Pal U, Wolgemuth CW, Eggers CH, Balic A, Radolf JD. 2009.
891 Live imaging reveals a biphasic mode of dissemination of *Borrelia burgdorferi* within ticks. *J*
892 *Clin Invest* 119:3652–3665. doi:10.1172/jci39401

893 Dynerman D, Lyden A, Quan J, Caldera S, McGeever A, Dimitrov B, King R, Cirolia G, Tan M,
894 Sit R, van den Berge M, Kerstjens HAM, Faiz A, Christenson S, Langelier C, DeRisi J,
895 Crawford E. 2020. Designing and implementing programmable depletion in sequencing
896 libraries with DASHit. *Biorxiv* 2020.01.12.891176. doi:10.1101/2020.01.12.891176

897 Edgar R, Domrachev M, Lash AE. 2002. Gene Expression Omnibus: NCBI gene expression
898 and hybridization array data repository. *Nucleic Acids Res* 30:207–210.
899 doi:10.1093/nar/30.1.207

900 Eggers CH, Samuels DS. 1999. Molecular evidence for a new bacteriophage of *Borrelia*
901 *burgdorferi*. *J Bacteriol* 181:7308–7313. doi:10.1128/jb.181.23.7308-7313.1999

902 Fraser CM, Casjens S, Huang WM, Sutton GG, Clayton R, Lathigra R, White O, Ketchum KA,
903 Dodson R, Hickey EK, Gwinn M, Dougherty B, Tomb J-F, Fleischmann RD, Richardson D,
904 Peterson J, Kerlavage AR, Quackenbush J, Salzberg S, Hanson M, van Vugt R, Palmer N,
905 Adams MD, Gocayne J, Weidman J, Utterback T, Watthey L, McDonald L, Artiach P,
906 Bowman C, Garland S, Fujii C, Cotton MD, Horst K, Roberts K, Hatch B, Smith HO, Venter
907 JC. 1997. Genomic sequence of a Lyme disease spirochaete, *Borrelia burgdorferi*. *Nature*
908 390:580–586. doi:10.1038/37551

909 Gilmore RD, Howison RR, Dietrich G, Patton TG, Clifton DR, Carroll JA. 2010. The *bba64* gene
910 of *Borrelia burgdorferi*, the Lyme disease agent, is critical for mammalian infection via tick
911 bite transmission. *P Natl Acad Sci Usa* 107:7515–7520. doi:10.1073/pnas.1000268107

912 Gilmore RD, Mbow ML, Stevenson B. 2001. Analysis of *Borrelia burgdorferi* gene expression
913 during life cycle phases of the tick vector *Ixodes scapularis*. *Microbes Infect* 3:799–808.
914 doi:10.1016/s1286-4579(01)01435-6

915 Grassmann AA, Tokarz R, Golino C, McLain MA, Groshong AM, Radolf JD, Caimano MJ. 2023.
916 BosR and PlzA reciprocally regulate RpoS function to sustain *Borrelia burgdorferi* in ticks
917 and mammals. *J Clin Invest* 133. doi:10.1172/jci166710

918 Gu W, Crawford ED, O'Donovan BD, Wilson MR, Chow ED, Retallack H, DeRisi JL. 2016.
919 Depletion of Abundant Sequences by Hybridization (DASH): using Cas9 to remove
920 unwanted high-abundance species in sequencing libraries and molecular counting
921 applications. *Genome Biol* 17:41. doi:10.1186/s13059-016-0904-5

922 Haas BJ, Chin M, Nusbaum C, Birren BW, Livny J. 2012. How deep is deep enough for RNA-
923 Seq profiling of bacterial transcriptomes? *Bmc Genomics* 13:734. doi:10.1186/1471-2164-13-
924 734

925 He M, Ouyang Z, Troxell B, Xu H, Moh A, Piesman J, Norgard MV, Gomelsky M, Yang XF.
926 2011. Cyclic di-GMP is Essential for the Survival of the Lyme Disease Spirochete in Ticks.
927 *Plos Pathog* 7:e1002133. doi:10.1371/journal.ppat.1002133

928 Hübner A, Yang X, Nolen DM, Popova TG, Cabello FC, Norgard MV. 2001. Expression of
929 *Borrelia burgdorferi* OspC and DbpA is controlled by a RpoN–RpoS regulatory pathway. *Proc*
930 *National Acad Sci* 98:12724–12729. doi:10.1073/pnas.231442498

931 Iyer R, Caimano MJ, Luthra A, Axline D Jr, Corona A, Iacobas DA, Radolf JD, Schwartz I. 2015.
932 Stage-specific global alterations in the transcriptomes of Lyme disease spirochetes during
933 tick feeding and following mammalian host adaptation. *Mol Microbiol* 95:509–538.
934 doi:10.1111/mmi.12882

935 Kalantar KL, Carvalho T, de Bourcy CFA, Dimitrov B, Dingle G, Egger R, Han J, Holmes OB,
936 Juan Y-F, King R, Kislyuk A, Lin MF, Mariano M, Morse T, Reynoso LV, Cruz DR, Sheu J,
937 Tang J, Wang J, Zhang MA, Zhong E, Ahyong V, Lay S, Chea S, Bohl JA, Manning JE, Tato
938 CM, DeRisi JL. 2020. IDseq—An open source cloud-based pipeline and analysis service for
939 metagenomic pathogen detection and monitoring. *Gigascience* 9:giaa111.
940 doi:10.1093/gigascience/giaa111

941 Kasumba IN, Bestor A, Tilly K, Rosa PA. 2016. Virulence of the Lyme disease spirochete before
942 and after the tick bloodmeal: a quantitative assessment. *Parasite Vector* 9:129.
943 doi:10.1186/s13071-016-1380-1

944 Kenedy MR, Lenhart TR, Akins DR. 2012. The role of *Borrelia burgdorferi* outer surface
945 proteins. *Fems Immunol Medical Microbiol* 66:1–19. doi:10.1111/j.1574-695x.2012.00980.x

946 Kovacs-Simon A, Titball RW, Michell SL. 2010. Lipoproteins of Bacterial Pathogens. *Infect*
947 *Immun* 79:548–561. doi:10.1128/iai.00682-10

948 Kung F, Anguita J, Pal U. 2013. *Borrelia burgdorferi* and tick proteins supporting pathogen
949 persistence in the vector. *Future Microbiol* 8:41–56. doi:10.2217/fmb.12.121

950 Kurokawa C, Lynn GE, Pedra JHF, Pal U, Narasimhan S, Fikrig E. 2020. Interactions between
951 *Borrelia burgdorferi* and ticks. *Nat Rev Microbiol* 18:587–600. doi:10.1038/s41579-020-0400-
952 5

953 Langmead B, Salzberg SL. 2012. Fast gapped-read alignment with Bowtie 2. *Nat Methods*
954 9:357–359. doi:10.1038/nmeth.1923

955 Love MI, Huber W, Anders S. 2014. Moderated estimation of fold change and dispersion for
956 RNA-seq data with DESeq2. *Genome Biol* 15:550. doi:10.1186/s13059-014-0550-8

957 Lyden A, Crawford E, Quan J, Caldera S, Dynerman D. 2019a. DASH Protocol v4.
958 doi:10.17504/protocols.io.6rjhd4n

959 Lyden A, Crawford E, Quan J, Caldera S, Pesce-Ares L. 2019b. In Vitro Transcription for
960 dgRNA v2. doi:10.17504/protocols.io.3bpgimn

961 Manning JE, Cantaert T. 2019. Time to Micromanage the Pathogen-Host-Vector Interface:
962 Considerations for Vaccine Development. *Nato Adv Sci Inst Se* 7:10.
963 doi:10.3390/vaccines7010010

964 Martin M. 2011. Cutadapt removes adapter sequences from high-throughput sequencing reads.
965 *Embnet J* 17:10–12. doi:10.14806/ej.17.1.200

966 Mi H, Muruganujan A, Huang X, Ebert D, Mills C, Guo X, Thomas PD. 2019. Protocol Update for
967 large-scale genome and gene function analysis with the PANTHER classification system
968 (v.14.0). *Nat Protoc* 14:703–721. doi:10.1038/s41596-019-0128-8

969 Miller JR, Koren S, Dilley KA, Harkins DA, Stockwell TB, Shabman RS, Sutton GG. 2018. A
970 draft genome sequence for the *Ixodes scapularis* cell line, ISE6. [version 1; peer review: 2
971 approved]. *F1000research* 7:297. doi:10.12688/f1000research.13635.1

972 Narasimhan S, Santiago F, Koski RA, Brei B, Anderson JF, Fish D, Fikrig E. 2002. Examination
973 of the *Borrelia burgdorferi* Transcriptome in *Ixodes scapularis* during Feeding. *J Bacteriol*
974 184:3122–3125. doi:10.1128/jb.184.11.3122-3125.2002

975 Ohnishi J, Piesman J, de Silva AM. 2001. Antigenic and genetic heterogeneity of *Borrelia*
976 *burgdorferi* populations transmitted by ticks. *Proceedings of the National Academy of*
977 *Sciences* 98:670–675. doi:10.1073/pnas.98.2.670

978 Ojaimi C, Brooks C, Casjens S, Rosa P, Elias A, Barbour A, Jasinskas A, Benach J, Katona L,
979 Radolf J, Caimano M, Skare J, Swingle K, Akins D, Schwartz I. 2003. Profiling of
980 Temperature-Induced Changes in *Borrelia burgdorferi* Gene Expression by Using Whole
981 Genome Arrays. *Infect Immun* 71:1689–1705. doi:10.1128/iai.71.4.1689-1705.2003

982 Ojaimi C, Mulay V, Liveris D, Iyer R, Schwartz I. 2005. Comparative Transcriptional Profiling of
983 *Borrelia burgdorferi* Clinical Isolates Differing in Capacities for Hematogenous Dissemination.
984 *Infect Immun* 73:6791–6802. doi:10.1128/iai.73.10.6791-6802.2005

985 Ouyang Z, Narasimhan S, Neelakanta G, Kumar M, Pal U, Fikrig E, Norgard MV. 2012.
986 Activation of the RpoN-RpoS regulatory pathway during the enzootic life cycle of *Borrelia*
987 *burgdorferi*. *Bmc Microbiol* 12:44. doi:10.1186/1471-2180-12-44

988 Pal U, Kitsou C, Drecktrah D, Yaş OB, Fikrig E. 2021. Interactions Between Ticks and Lyme
989 Disease Spirochetes. *Curr Issues Mol Biol* 42:113–144. doi:10.21775/cimb.042.113

990 Pal U, Li X, Wang T, Montgomery RR, Ramamoorthi N, de Silva AM, Bao F, Yang X, Pypaert M,
991 Pradhan D, Kantor FS, Telford S, Anderson JF, Fikrig E. 2004. TROSPA, an *Ixodes*
992 *scapularis Receptor* for *Borrelia burgdorferi*. *Cell* 119:457–468.
993 doi:10.1016/j.cell.2004.10.027

994 Patro R, Duggal G, Love MI, Irizarry RA, Kingsford C. 2017. Salmon provides fast and bias-
995 aware quantification of transcript expression. *Nat Methods* 14:417–419.
996 doi:10.1038/nmeth.4197

997 Patton TG, Brandt KS, Nolder C, Clifton DR, Carroll JA, Gilmore RD. 2013. *Borrelia burgdorferi*
998 *bba66* Gene Inactivation Results in Attenuated Mouse Infection by Tick Transmission. *Infect*
999 *Immun* 81:2488–2498. doi:10.1128/iai.00140-13

1000 Phelan JP, Kern A, Ramsey ME, Lundt ME, Sharma B, Lin T, Gao L, Norris SJ, Hyde JA, Skare
1001 JT, Hu LT. 2019. Genome-wide screen identifies novel genes required for *Borrelia*
1002 *burgdorferi* survival in its Ixodes tick vector. *Plos Pathog* 15:e1007644.
1003 doi:10.1371/journal.ppat.1007644

1004 Radolf JD, Caimano MJ, Stevenson B, Hu LT. 2012. Of ticks, mice and men: understanding the
1005 dual-host lifestyle of Lyme disease spirochaetes. *Nat Rev Microbiol* 10:87–99.
1006 doi:10.1038/nrmicro2714

1007 Rego ROM, Bestor A, Rosa PA. 2011. Defining the Plasmid-Borne Restriction-Modification
1008 Systems of the Lyme Disease Spirochete *Borrelia burgdorferi*. *J Bacteriol* 193:1161–1171.
1009 doi:10.1128/jb.01176-10

1010 Rego ROM, Bestor A, Štefka J, Rosa PA. 2014. Population Bottlenecks during the Infectious
1011 Cycle of the Lyme Disease Spirochete *Borrelia burgdorferi*. *Plos One* 9:e101009.
1012 doi:10.1371/journal.pone.0101009

1013 Revel AT, Talaat AM, Norgard MV. 2002. DNA microarray analysis of differential gene
1014 expression in *Borrelia burgdorferi*, the Lyme disease spirochete. *Proc National Acad Sci*
1015 99:1562–1567. doi:10.1073/pnas.032667699

1016 Ring K, Couper LI, Sapiro AL, Yarza F, Yang XF, Clay K, Mateusiak C, Chou S, Swei A. 2022.
1017 Host blood meal identity modifies vector gene expression and competency. *Mol Ecol*
1018 31:2698–2711. doi:10.1111/mec.16413

1019 Rosenberg R, Lindsey NP, Fischer M, Gregory CJ, Hinckley AF, Mead PS, Paz-Bailey G,
1020 Waterman SH, Drexler NA, Kersh GJ, Hooks H, Partridge SK, Visser SN, Beard CB,
1021 Petersen LR. 2018. Vital Signs: Trends in Reported Vectorborne Disease Cases — United
1022 States and Territories, 2004–2016. *Morbidity Mortal Wkly Rep* 67:496–501.
1023 doi:10.15585/mmwr.mm6717e1

1024 Samuels DS, Lybecker MC, Yang XF, Ouyang Z, Bourret TJ, Boyle WK, Stevenson B,
1025 Drecktrah D, Caimano MJ. 2021. Gene Regulation and Transcriptomics. *Curr Issues Mol Biol*
1026 42:223–266. doi:10.21775/cimb.042.223

1027 Schneider CA, Rasband WS, Eliceiri KW. 2012. NIH Image to ImageJ: 25 years of image
1028 analysis. *Nat Methods* 9:671–675. doi:10.1038/nmeth.2089

1029 Schwartz I, Margos G, Casjens SR, Qiu W-G, Eggers CH. 2021. Multipartite Genome of Lyme
1030 Disease *Borrelia* : Structure, Variation and Prophages. *Curr Issues Mol Biol* 42:409–454.
1031 doi:10.21775/cimb.042.409

1032 Shaw WR, Catteruccia F. 2018. Vector biology meets disease control: using basic research to
1033 fight vector-borne diseases. *Nat Microbiol* 4:20–34. doi:10.1038/s41564-018-0214-7

1034 Sonenshine DE, Anderson JM. 2014. Mouthparts And Digestive System In: Sonenshine DE,
1035 Roe RM, editors. Biology of Ticks. Oxford University Press. pp. 122–162.

1036 Spielman A, Ribeiro JMC, Mather TN, Piesman J. 1987. Dissemination and Salivary Delivery of
1037 Lyme Disease Spirochetes in Vector Ticks (Acari: Ixodidae). *J Med Entomol* 24:201–205.
1038 doi:10.1093/jmedent/24.2.201

1039 Steere AC, Sikand VK, Meurice F, Parenti DL, Fikrig E, Schoen RT, Nowakowski J, Schmid CH,
1040 Laukamp S, Buscarino C, Krause DS. 1998. Vaccination against Lyme Disease with
1041 Recombinant *Borrelia burgdorferi* Outer-Surface Lipoprotein A with Adjuvant. *New Engl J*
1042 *Medicine* 339:209–215. doi:10.1056/nejm199807233390401

1043 Steere AC, Strle F, Wormser GP, Hu LT, Branda JA, Hovius JWR, Li X, Mead PS. 2016. Lyme
1044 borreliosis. *Nat Rev Dis Primers* 2:16090. doi:10.1038/nrdp.2016.90

1045 Stevenson B, Zückert WR, Akins DR. 2000. Repetition, conservation, and variation: the multiple
1046 cp32 plasmids of *Borrelia* species. *J Mol Microb Biotech* 2:411–422.

1047 Thomas PD, Ebert D, Muruganujan A, Mushayahama T, Albou L-P, Mi H. 2022. PANTHER:
1048 Making genome-scale phylogenetics accessible to all. *Protein Sci* 31:8–22.
1049 doi:10.1002/pro.4218

1050 Tilly K, Rosa PA, Stewart PE. 2008. Biology of Infection with *Borrelia burgdorferi*. *Infect Dis Clin*
1051 *N Am* 22:217–234. doi:10.1016/j.idc.2007.12.013

1052 Tokarz R, Anderton JM, Katona LI, Benach JL. 2004. Combined Effects of Blood and
1053 Temperature Shift on *Borrelia burgdorferi* Gene Expression as Determined by Whole
1054 Genome DNA Array. *Infect Immun* 72:5419–5432. doi:10.1128/iai.72.9.5419-5432.2004

1055 Wachter J, Cheff B, Hillman C, Carracoi V, Dorward DW, Martens C, Barbian K, Nardone G,
1056 Olano LR, Kinnersley M, Secor PR, Rosa PA. 2023. Coupled induction of prophage and
1057 virulence factors during tick transmission of the Lyme disease spirochete. *Nat Commun*
1058 14:198. doi:10.1038/s41467-023-35897-3

1059 Zhang H, Marconi RT. 2005. Demonstration of Cotranscription and 1-Methyl-3-Nitroso-
1060 Nitroguanidine Induction of a 30-Gene Operon of *Borrelia burgdorferi*: Evidence that the 32-
1061 Kilobase Circular Plasmids Are Prophages. *J Bacteriol* 187:7985–7995.
1062 doi:10.1128/jb.187.23.7985-7995.2005

1063 Zhang L, Zhang Y, Adusumilli S, Liu L, Narasimhan S, Dai J, Zhao YO, Fikrig E. 2011.
1064 Molecular Interactions that Enable Movement of the Lyme Disease Agent from the Tick Gut
1065 into the Hemolymph. *Plos Pathog* 7:e1002079. doi:10.1371/journal.ppat.1002079

1066 Zhu A, Ibrahim JG, Love MI. 2018. Heavy-tailed prior distributions for sequence count data:
1067 removing the noise and preserving large differences. *Bioinformatics* 35:2084–2092.
1068 doi:10.1093/bioinformatics/bty895

1069